Late Cretaceous-Cenozoic basin inversion and palaeostress fields in the North Atlantic-western Alpine-Tethys realm: implications for intraplate tectonics

Randell Stephenson (University of Aberdeen), corresponding author (r.stephenson@abdn.ac.uk)
Christian Schiffer (Uppsala University)
Alex Peace (McMaster University)
Søren Bom Nielsen (Aarhus University)
Scott Jess (University of Calgary)

Abstract

Intraplate basin/structural inversion (indicating tectonic shortening) is a good marker of ("far-field") tectonic stress regime changes that are linked to plate geometries and interactions, a premise that is qualitatively well-established in the literature. There is also quantitative evidence that Late Cretaceous-Palaeocene inversion of sedimentary basins in north-central Europe was explicitly driven by an intraplate, relaxational response to forces developed during rapid reconfigurations of the Alpine-Tethys (Europe-Africa) convergent plate boundary. Although with a degree of temporal ambiguity, three main periods of intraplate tectonics (marked primarily by structural inversion in initially extensional sedimentary basins) are indicated in the North Atlantic-western Alpine-Tethys realm. These are in the Late Cretaceous-Palaeocene, the Eocene-Oligocene and the Miocene. Examples recording these periods are primarily interpreted seismic reflection profiles (of varying quality and resolution) from the published literature. Additional examples where seismic data are not present, but timing constraints are robust from other observations, have also been considered. The schematic distribution and orientation of the literature-compiled intraplate inversion structures are compared to the model palaeostress fields derived from Late Cretaceous-Palaeocene, Eocene-Oligocene and Miocene tectonic reconstructions of the North Atlantic-western Alpine-Tethys realm. The modelled palaeostress fields include geopotential effects from palaeobathymetry and palaeotopography of the Earth's surface as well as laterally variable lithosphere and crustal palaeo-thicknesses but do not include any component of the stress field produced by processes occurring at contiguous convergent plate margins. The former satisfactorily provides the background stress field of most of the Earth's plate interiors and it is inferred that the latter is paramount in producing "stress trauma" in the interior of plates resulting in permanent intraplate deformation such as basin inversion.

Keywords: intraplate deformation, basin inversion, continental lithosphere, lithosphere stress, North Atlantic, Alpine-Tethys belt

1. Introduction

1.1 Background and premise

Most tectonic deformation recorded at or near the Earth's surface is understood to have occurred near plate boundaries (where oceanic lithosphere is subducted, plates collide and are sutured to form orogenic belts) or near proto-plate boundaries (where lithosphere rifting forms major

sedimentary basins and eventually, after plate rupturing, new passive continental margins). There is, nevertheless, a widespread geological record of significant tectonic deformation that has occurred well removed from plate boundaries (e.g. Ziegler, 1988; Ziegler, 1990; Hand and Sandiford, 1999; Banerjee et al., 2008; Sandiford and Quigley, 2009; Lu et al., 2013; Raimondo et al., 2014) not to mention abundant present-day seismicity (e.g. Johnston, 1996; Hurd and Zoback, 2012; Talwani, 2014; Mazotti et al., 2018) in specific intraplate settings.

The study of intraplate compressional deformation structures, particularly those of latest Cretaceous-early Palaeocene age, has a long history in Europe (e.g. Voigt, 1962; van Hoorne, 1987; Ziegler, 1988; Ziegler, 1990; Kockel, 2003; Marotta and Sabadini, 2003; Kley and Voight, 2008; Kley, 2018). Ziegler (1987) and Ziegler et al. (1995; 2002; 2006) placed the genesis of these European structures into a plate tectonic framework involving processes at the Europe-Africa plate boundary, as did Sandiford and Quigley (2009) for intraplate deformation in the Australian continent in the context of plate interactions between the Australian plate and those adjoining it. The transmission of these stresses from plate boundary to plate interior implies a strong continental lithosphere and, conversely, the presence of favourably orientated inherited structural or thermo-mechanical lithosphere weaknesses to localise their relaxation by causing intraplate strain (Nielsen et al., 2005; Stephenson et al., 2009; Raimondo et al., 2014). Of course, processes at convergent plate boundaries (related broadly to “slab pull” and ambient effects) are not the only sources of the intraplate lithosphere stress field (e.g. Ranalli, 1995). The transient effects of ice sheets, especially the relaxation of lithosphere after their removal, are, for example, evidently responsible for some present-day seismicity in northern Europe and Canada (Muir-Wood, 2000; Sella et al., 2007). More important in the present context are changes in crustal and lithosphere thickness as well as the presence of topography (or bathymetry) at the top of the lithosphere, including the uplift of lithosphere at mid-ocean ridges (“ridge push”) also make significant contributions to the lithosphere stress state. This component of stress is due to the lithosphere’s geopotential energy gradients (e.g. Artyushkov, 1973) and can be referred to as the geopotential stress field of the lithosphere and it is possible to compute an estimate of this in the geological past (e.g. Peace et al., 2018a; Schiffer et al., 2018) utilising modelled palaeotectonic reconstructions (e.g. Seton et al., 2012).

Accordingly, the premise of this paper is that the generation of intraplate deformation is a good indicator of key “far-field” tectonic stress regime changes that are linked to important and probably geologically abrupt plate boundary reorganisations and superimposed upon the geopotential stress field of the lithosphere. An examination of the style and timing of intraplate deformation structures in the North Atlantic-western Tethys realm, in the context of the evolving plate tectonic regime and geopotential stress field from the Late Cretaceous through the Cenozoic, may therefore illuminate

76 critical issues to do with underlying driving geodynamic processes and how these occur at plate
77 boundaries. The existence of an underlying template of pre-existing structures and lateral
78 heterogeneities in the crust and lithosphere and the effects of inheritance that these impose upon
79 later intraplate deformation is a "given" within the scope of the present study.

80 *1.2 Timing of intraplate deformation: basin inversion*

81 Present-day intraplate deformation is signified succinctly by seismicity (e.g. Calais et al., 2016) but
82 intraplate deformation in the geological past can only be inferred if structural relationships
83 demonstrating that deformation has taken place are preserved and observable. However, the timing
84 of deformation and even its style (shortening or extensional) can be extremely difficult or even
85 impossible to decipher if, for example, the deformed strata consist of crystalline Precambrian
86 basement rocks and the age of the deformation was Cenozoic. Unfortunately, in this regard, large
87 parts of continental interiors are composed of crystalline Precambrian basement rocks lying at or
88 near the surface. In contrast, where sedimentary strata overlie basement rocks in continental
89 interiors, they typically provide a good record of style and timing of tectonic deformation because of
90 the range of ages that are potentially (but not always precisely) preserved in the sedimentary
91 stratigraphy.

92 "Basin inversion" manifests the upper and supracrustal expression of compressional intraplate
93 deformation as mild folding, uplift and reverse faulting of sedimentary basins formed in intraplate
94 settings. It occurs where intraplate sedimentary basins initially formed under extensional or
95 transtensional conditions are subsequently structurally inverted by the effects of a later
96 compressional or transpressional stress regime. The typical expression of "basin inversion",
97 preserved within the stratigraphic succession of a sedimentary basin – hence with the timing of
98 inversion well recorded if the age of the stratigraphy is known – is shown in Figure 1. The faults in the
99 deeper part of the section have the kinematic appearance of normal faults and were clearly forming
100 during tectonic extension, indicated by the thicker sedimentary package on the hanging wall side of
101 the fault compared to the footwall side. However, later, the fault as a whole has been reactivated as
102 a reverse fault and displays reverse fault kinematics in the shallower part of the section. The
103 antiformal structure in the post-rift succession as well as the presence of the "syn-inversional"
104 depocentre associated with the anticline are also typical attributes of "basin inversion". If the
105 antiformal structure and/or inverted faults are exposed at the surface then the term "basin
106 inversion" describes the process when elongate stretches of a former area with sedimentary infill
107 reverses its vertical direction of movement and becomes uplifted and eroded (Ziegler, 1987).

"Basin inversion" accordingly provides not only an explicit record of compressional intraplate deformation but a good expectation of determining the timing of this deformation, or at least bracketing its time depending on the preserved sedimentary succession.

1.3 Approach: geopotential palaeostress compared to distribution of intraplate deformation in the North Atlantic-western Alpine-Tethys realm

Focusing on intraplate basin inversion structures implies that the observational database will predominantly be derived from "failed rift" basins formed away from plate boundaries prior to and possibly in the early stages of extension that led to continental break-up in the North Atlantic. They were subsequently placed into a regime of tectonic compression with shortening as a result. In this regard, basin inversion structures and associated features are fairly abundant in the North Atlantic-western Alpine-Tethys realm study area because they have typically reactivated widely distributed Late Palaeozoic-Mesozoic sedimentary basins and rifts that had formed during the relaxation of lithosphere accreted during the Palaeozoic Caledonian and Variscan orogenies in the area and the ensuing onset of the break-up of Pangaea (Ziegler et al., 1995; Ziegler et al., 2006; Gutiérrez-Alonso et al., 2008).

One of the aims of this paper is to examine the basin inversion information compiled in the Ziegler atlases (Ziegler, 1988; 1990) and add to this the marine areas of the North Atlantic where new information has become available in the meantime. A large body of relevant published literature is reviewed in section 2. Examples showing how basin inversion is differently expressed and how it occurs at different times within the study realm are included, the examples being derived from interpreted seismic reflection profiles.

The objectives of the present work are, however, not only to examine where and when intraplate deformation took place in the study realm but also to compare its style and timing with models of intraplate palaeostress regimes at the tectonically active times. Stresses in the lithosphere (e.g. Ranalli, 1995; Doglioni and Panza, 2016) are produced by a variety of sources, including processes like slab pull and shear resistance at collisional plate boundaries (and convective processes instigated by subduction) and shear resistance at transform plate boundaries; horizontal gradients of lithospheric potential energy (including "ridge push" and variations in lithosphere and crustal thicknesses and other lateral density changes) and horizontal gradients of pressure variations at the base of the lithosphere. The last of these gives rise to "dynamic topography" as a quasi-isostatic response to density variations in the asthenosphere, but not to the effects of a flowing sub-lithospheric mantle with vertical momentum (e.g. Molnar et al., 2015). The latter might also be present if lithosphere is moving discretely with respect to the underlying mantle (e.g. Chalot-Prat et

al., 2016) and there may also be convective drag at the base of the lithosphere although this remains a matter of some uncertainty (e.g. Lithgow-Bertelloni and Guynn, 2004; Ghosh et al., 2008; Höink et al., 2011). Much of this can be considered as stress caused by "plate boundary processes" with those generated at collisional plate boundaries being extremely complex in contrast to those produced by "ridge push" at mid-oceanic accretionary plate boundaries. The latter contributes to what is referred to the geopotential (GP) stress field, which is primarily cause by lateral density variations in the lithosphere and sub-lithospheric upper mantle. It is known that the GP stresses tend to dominate plate interiors in the absence of those derived from complex plate boundary effects (e.g. Nielsen et al., 2014).

GP stresses can be computed for Late Cretaceous-Cenozoic tectonic settings with some degree of confidence because of the regionality of the rheological response to these stresses and because there exist robust reconstructions, and, with these, good estimates of oceanic and continental lithosphere thickness and density structure, necessary for calculation of the moment of the density distribution. In contrast, it is very difficult – or would indeed become "ad hoc" – to incorporate the complex effects of collisional plate boundary processes into the palaeostress fields; there are many relatively more poorly understood contributing factors. These may be highly transient and competing with one another and doing so in a more limited volume of the Earth, but over greater depths and, therefore, with a much broader and more complex rheological response.

In the present work, for this reason, it is the GP palaeostress fields that are computed for times at which intraplate deformation characterises the North Atlantic-western Alpine-Tethys realm. The methodology of how this is done for the palaeotectonic regimes characterising the study is presented in section 3.

The geological (observational) and modelling (theoretical) results are presented and compared in section 4. The observational evidence of intraplate deformation reviewed in section 2 comprises a complex array of small pieces of information categorised in terms of their ages as precisely as possible, but not often not very precisely at all, by a variety of authors using a variety of methods. The modelled palaeostress fields are, in contrast, smooth, displaying variability only at a tectonically regional scale relevant to uncertainties inherent to their boundary conditions and input data. Accordingly, a degree of simplification, averaging and stylisation of the former (in both space and time), during which detailed information is lost but its significance hopefully retained, is applied in order to create generalised images of the inversion tectonics for comparison to modelled palaeostress regimes at different time steps.

Section 5 provides a comprehensive review of the background and implications of the integrated basin inversion and palaeostress regime results in the study realm in terms of stress state and rheology of continental lithosphere and their regional and global plate tectonic context.

2. Basin inversion in the North Atlantic-western Tethys realm: observations

A compilation of intraplate basin inversion structures and their ages of formation in the North Atlantic-western Tethys realm has been made on the basis of an extensive survey of the published literature, sub-divided into five geographic sub-realms outlined in Figure 2a: (1) Baffin-Labrador seas and the adjacent onshore, (2) Greenland and Barents seas and the adjacent North Atlantic onshore, (3) the Norwegian and Ireland-Great Britain continental margins, (4) onshore west-central Europe including Ireland-Great Britain and their contiguous continental seas) and, last, (5) onshore eastern Europe, including the Black Sea. Several examples are included (Figures 3-8, located in Figure 2a) to give an idea about the different ways in which basin inversion is expressed in the study realm but also as an illustration of the range of ages at which these basin inversion structures are reported to have formed.

2.1 Labrador Sea-West Greenland-Baffin Bay (including Ellesmere Island)

Compressive structures dating from the mid-Cenozoic are apparent across both the onshore and offshore domains of the Davis Strait (between Labrador Sea and Baffin Bay), though remain poorly explored and difficult to properly characterise. On the northwest Greenland margin, a number of inversion structures are observed doming overlying Eocene strata (Gregersen et al., 2013), with Whittaker et al. (1997) suggesting inversion in this area took place at latest Palaeocene and early Eocene time. Further south, adjacent to the Ungava Fault Zone (UFZ; Fig. 2b), which connects the Labrador Sea and Baffin Bay through Davis Strait, Figure 3 shows a number of major inversion structures and minor thrust faults and folds triggered by Eocene transpressional fault reactivation (Peace et al., 2018b). There is also some onshore evidence for reactivation, but timings are very poorly constrained in west Greenland and Labrador (Wilson et al., 2006; Peace et al., 2018a). Field mapping and seismic data from this part of the west Greenland margin onshore indicate inversion of faults following the end of major volcanism in the Palaeocene (Skaarup and Pulvertaft, 2007) and photogrammetric mapping of volcanic surfaces highlights an undulating morphology adjacent to major basin faults, implying post-Palaeocene inversion (Sørensen et al., 2017).

The region north of Baffin Bay, in northernmost Greenland and adjacent islands of the Canadian High Arctic, has been strongly deformed during the intraplate Eurekan Orogen (Fig. 2b; e.g. Piepjohn et al.,

2018). It occurred as the result of a noted reorientation of ocean spreading in Baffin Bay (Oakey and Chalmers, 2012; Døssing et al., 2013; Hosseinpour et al., 2013) in the Eocene concomitant with a rotation of the movement of Greenland relative to northern Canada and leading to convergence and some tens up to one hundred kilometres of crustal shortening (cf. Stephenson et al., 2018) and which was shown by Welford et al. (2018) using deformable plate models to result in substantial crustal thickening in northeast Greenland. In this regard the Eurekan Orogen itself, the main tectonic element of which comprises a crustal-scale pop-up structure, represents a profound case of intraplate deformation involving basin inversion (Stephenson et al., 2018).

2.2 Barents Sea and East Greenland margin

The subsurface geology of the Barents Sea is better known, than much of the rest of the offshore part of the study realm, much of which has essentially no data coverage at all. Although this gives a geographical sampling/mapping bias, it has provided comparatively better images of inversion structures and, most importantly, estimates of their ages. The published literature reveals a complex image of basin inversion in the western Barents Sea (BaS; Fig. 2a) and around Svalbard (Sv; Fig. 2a). Numerous structures display inversion in the Late Jurassic-Cretaceous (e.g. Gabrielsen et al., 1990; Gabrielsen and Færseth, 1988; Vågnes et al., 1998) although these are not of direct interest in the present context. However, many of them, in turn, were compressionally reactivated in the Palaeocene, Eocene-Oligocene and Miocene. The Greenland Sea (GS; Fig. 2a) on the northeast Greenland margin shows a broadly similar geological and tectonic history and Figure 4 shows an example of post-Palaeogene inversion in a transpressional setting on the northeast Greenland Shelf (e.g. Lundin and Doré, 2002; Hamann et al., 2005; Svennevig et al., 2016; Schack-Pedersen and Håkansson, 2001).

A major phase of basin inversion occurred in this area in the Cenozoic (Gabrielsen et al., 1990; Vågnes et al., 1998), but many reported examples have poor age control and are often simply identified as “Tertiary” or “Late Cretaceous-Tertiary” or “Late-Cretaceous-early Tertiary” (Gabrielsen et al., 1997). In some cases more detailed age control is available: Brekke and Riis (1987), Faleide et al. (1993) and Sund et al. (1986) all report “Late Palaeocene” or “Palaeocene” for various inversion structures; others report “early Tertiary” (e.g. Koehl et al., 2018), Eocene (Gabrielsen et al., 1990, Ryseth et al., 2003; Sund et al., 1986) or “Miocene inversion” (Sættem et al., 1994; Ur Rehman, 2012; Henriksen et al., 2011; Blaich et al., 2017).

Many structural highs and fault zones/complexes along the western Barents Sea margin show evidence for single or multiple inversion events within the studied late Cretaceous to Miocene time interval (e.g. Brekke and Riis, 1987; Faleide et al., 1993; Sund et al., 1986; Faleide et al., 1993; Koehl

et al., 2018; Breivik et al., 1998; Gabrielsen et al., 1990; Ryseth et al., 2003). Many of the same structures also display what has been interpreted as Eocene and/or Miocene inversional processes, indicating that structural reactivation in the Barents Sea has been highly sensitive to evolving regional stress fields.

2.3 Norwegian and Ireland-Great Britain continental margins

Major structures with doming of sedimentary strata dating from the Palaeocene, Eocene, Miocene or Pliocene are present across much of the central Norwegian margin, suggesting that a widespread and episodic compressional regime was present during much of the Cenozoic (Doré et al., 2008; Kimbell et al., 2016). One such structure lying within the Vøring Basin (VB; Fig. 2b) exemplifies the tectonic inversion across the Norwegian shelf (Fig. 5). Lundin and Doré (2002) recognised active compression from the mid-Eocene to the early Miocene with diachronous formation from the SW to NE during this time. The source of doming across the feature is believed to be the inversion of a Jurassic-aged fault complex that aligns with the northern fold limb of the anticline (Doré and Lundin, 1996).

A number of offshore studies have outlined significant episodes of compression along the whole of the Ireland-Great Britain continental shelf region, including elements such as the Faroe-Shetland Basin (FSB; Fig. 2b) north of Scotland southeast into the Rockall Basin (RB; Fig. 2b), northwest and west of Scotland and north and northwest of Ireland (e.g. Boldreel and Andersen, 1993; Boldreel and Andersen, 1998; Andersen et al., 2000; Mosar et al., 2002; Johnson et al., 2005; Kimbell et al., 2016; Stoker et al., 2017). Observable fault inversions and folding in this area are believed to have formed at a variety of intervals during the Late Palaeocene to Early Eocene (Boldreel and Andersen, 1998), Early to Mid-Eocene (Johnsen et al., 2005), Oligocene to Miocene (Boldreel and Andersen, 1998) and Early to Mid-Miocene (Andersen et al., 2000; Ritchie et al., 2008). A number of domal features in the region are sourced from reactivation of underlying Caledonian basement lineaments (Ritchie et al., 2008). Compressional features on the northwestern margin of the Hatton Basin (Hatton Bank) are believed to have initiated in the Late-Eocene, implied by the presence of thinning Ypresian sediments and a Mid-Eocene unconformity and likely linked to changes in seafloor spreading (Boldreel and Andersen, 1998; Johnson et al., 2005). Figure 6 shows part of a seismic profile in the northeasternmost part of the Rockall Basin displaying significant inversion in the Eocene. Johnson et al. (2005) also consider there to be evidence of a major phase of early to mid-Miocene fold growth in this area.

2.4 West-central continental Europe (including Ireland and Great Britain and the Irish and North seas)

Widespread inversion is documented across Great Britain and Ireland and its contiguous continental marine areas. Williams et al. (2005) present evidence offshore Wales in the Irish Sea for two

significant inversion episodes in the Late Cretaceous and the Neogene. Further south, In the Celtic Sea Basin, Rodríguez-Salgado et al. (2017) report "Oligocene-Miocene" inversion structures. Le Breton et al. (2012) identified sinistral reactivation of the Great Glen Fault during the period 36-26 Ma (Eocene-Oligocene) although no basin inversion is displayed in this case. Across southern Great Britain and in the southern North Sea, basin inversion is widespread, much of it displaying Late Cretaceous-Palaeocene timing (e.g. Chesher, 1991; Blundell, 2002).

Eocene-aged inversion has been noted immediately off the southern coast of Great Britain (Underhill and Paterson, 1998) and Late Cretaceous-Palaeocene as well as Eocene-Oligocene inversional phases are recorded in the Broad Fourteens Basin (BFB; Fig. 2b) in the Dutch sector of the southern North Sea (de Lugt et al., 2003) as well as throughout onshore Netherlands (de Jager, 2003). These authors and the Dutch literature generally refer to the Eocene-Oligocene event as "Pyrenean". Former basin bounding faults of the proto-Pyrenees deep basin were inverted at this time (Pedrera et al., 2017; Izquierdo-Llavall et al., 2020), although inversion started in the Late Cretaceous according to Dielforder et al. (2019), with the Pyrenees Orogen (PO; Fig. 2b) itself now mainly recognised as forming in an intraplate setting (i.e., in the absence of a subduction plate boundary).

The Tornquist-Tesseyre Zone (TTZ; Fig. 2b) runs across continental Europe from the northeastern North Sea over the Baltic sea, where it is more frequently referred to as the Sorgenfrei-Tornquist Zone (STZ; Fig. 2b) and north-central Europe until being hidden beneath the eastern Carpathians has acted as the tectonic buffer zone between the East European Craton (EEC; Fig. 2b) to its east-northeast and more mobile European lithosphere to the west-southwest. It originated as the passive margin of proto-continent Baltica (now preserved as the EEC) in the Neoproterozoic. Later it became the locus of accretion of other terranes to Europe during the Palaeozoic Caledonian and Variscan orogens. From probably the Late Carboniferous-Early Permian (Mogensen, 1994; Mogensen and Korstgård, 2003; Erlström et al., 1997) it has been a zone of structural weakness that has readily responded by both transtensional and transpressional deformations to in-plane stress changes. During the late Cretaceous-Palaeocene particularly well documented examples of the deformation styles associated with basin inversion can be observed (Ziegler, 1988, 1990; Ziegler et al., 1995; Vejbæk and Andersen, 1987; 2002; Dadlez et al., 1995; Scheck-Wenderoth et al., 2008; Krzywiec and Stachowska, 2016), as illustrated in Figure 7.

2.5 Eastern continental Europe (including the Black Sea)

Ziegler (1990) considered that Late Cretaceous(-Palaeocene) inversion on the TTZ reflected a change in stress regime from Pangaean break-up (transtensional) to the transpressional regime produced by the onset of the Eo-Alpine orogenic phase in north-central Europe and, as such, intrinsically linked to

304 inheritance of late Palaeozoic structures, restricted to the TTZ itself and the Palaeozoic accreted
305 crustal terranes to its west-southwest (Fig. 2b). However, it has been subsequently documented that
306 inversion of the Donbas Foldbelt (DF; Fig. 2b) in Ukraine and southern Russia, previously thought to
307 have been similarly of late Palaeozoic age (cf. Stephenson et al., 1993), is also late Cretaceous-
308 Palaeocene (e.g. Stovba and Stephenson, 1999; Maystrenko et al., 2003; Saintot et al., 2003ab). The
309 style of Late Cretaceous-Palaeocene inversion in the case of the Donbas, embedded as it is in the
310 Archaean-Palaeoproterozoic lithosphere of the EEC is notable in that it involves a compressional pop-
311 up ("flower structure") formed at a crustal-scale (Maystrenko et al., 2003) and has likely been
312 localised not by specific structural heterogeneities but by thermal heterogeneities caused by the
313 presence of the thick Late Palaeozoic and younger sedimentary basin itself (Stephenson et al., 2009).

314 Although there is no strong evidence of inversion younger than Palaeocene in the Donbas Foldbelt,
315 younger basins such as those of the Black Sea were inverted in the Eocene-Oligocene and later in the
316 Miocene (Khriachtchevskaia et al., 2010). Figure 8 shows an example of Miocene inversion from the
317 northern margin of the Black Sea, just offshore the Crimean Peninsula (CF; Fig. 2a). Sheremet et al.
318 (2019) suggested that Black Sea inversion, as expressed in the contiguous southern Crimean
319 highlands began as early as Late Palaeocene. These highlands represent the western prolongation of
320 the Greater Caucasus Orogen (GCO; Fig. 2b), which is now, like the Pyrenees, also generally
321 considered to have formed in an intraplate setting (e.g. Saintot et al., 2006; Sosson et al., 2016).
322 Given the peri-cratonic setting of the Crimean-Caucasus orogenic belt and contiguous northern
323 margin of the Black Sea (e.g. Starostenko et al., 2016), these areas are included in the current
324 overview of intraplate deformation within North Atlantic-western Alpine-Tethys realm, but
325 deformation in the more mobile parts of the active Tethys belt are not considered further.

326 *2.6 Regional and temporal patterns of basin inversion and intraplate deformation in the North*
327 *Atlantic-western Alpine-Tethys study realm: summary*

328 The intraplate deformation in the form of basin inversion and associated folding in the study area
329 shows an identifiable temporal-spatial pattern (despite being limited by incomplete "sampling", a
330 possible bias towards evidence in well-studied areas and sometimes fairly ambiguous timing
331 constraints). Within these constraints, basin inversion was focused in north-central Europe during
332 the Late Cretaceous-Palaeocene with a prominent NE-SW orientation (shortening direction) with
333 many examples from the Tornquist-Tesseyre Zone and environs, central and eastern Europe, as well
334 as the North Sea and contiguous areas. After North Atlantic break-up, in the Eocene-Oligocene,
335 intraplate deformation shifted from west-central Europe northwestwards and southwards. It became
336 dominantly focused on the Norwegian Sea shelf, Baffin Bay/Davis Strait and, most prominently

Ellesmere Island, North Greenland and the Barents Sea/Svalbard. There is some evidence for Eocene-Oligocene basin inversion in north-central Europe and some inversion structures are seen in the northern periphery of the Alpine collision zone (cf. Alpine deformation Front – ADF; Fig. 2b) and in the Greater Caucasus/Black Sea area. In the Miocene, only minor inversion is reported from the Norwegian margin and Barents Sea, but more clearly from southern Great Britain and in the eastern part of the study area.

The literature review suggests that there are key periods of tectonic transition marked by intraplate deformation in the North Atlantic-western Alpine-Tethys realm since the Late Cretaceous. Although precise timing is often difficult to ascertain, the available observations suggest that much of it, perhaps all, is clustered during three key periods, these being the Late Cretaceous-Palaeocene, Eocene-Oligocene and Miocene. Figure 9 presents a schematic representation of the published results plotted according to palaeo-geographic plate reconstructions relevant to these three key periods based on the PALEOMAP PaleoAtlas for GPlates of Scotese (2016). The maps in Figure 9 are not intended as atlases. The locations of intraplate deformation symbols are generalised within the peripheral regions they are plotted, both in position and orientation. The geological ages of each map are correct for the reconstructed palaeo-geography but the geological elements portrayed thereon are reported in the literature to be spanning the whole of the respective geological periods indicated. Given the intrinsic ambiguity in much of the relevant literature, there is also some degree of interpretation in the maps as presented.

3. Geopotential palaeostress regimes in the North Atlantic-western Tethys realm

3.1 Principles and computational approach

Geopotential (GP) stresses arise from horizontal gradients in geopotential energy (GPE) per unit area, the integral over the vertical column of a lithostatic pressure anomaly that is defined by:

$$GPE = \int_{-H}^{L} (L - z)\Delta\rho g \, dz$$

where z is depth, L is the reference depth (up to which density variations are incorporated), H the topographic elevation, $\Delta\rho$ is the vertical density anomaly with respect to a reference lithosphere, and g is the gravitational acceleration at Earth's surface (e.g. Artyushkov, 1973; Coblentz et al., 1995;

Fleitout and Froidevaux, 1983). The reference depth (*L*) is taken as 100 km, as an approximation of the elastic layer of the Earth's lithosphere that supports and transmits stresses, following Flesch et al. (2001) and Ghosh et al. (2008). The geopotential stresses as defined can generally account for large parts of the intraplate stress field and may be considered as a good approximation of the ambient stress state of the plates, superimposed onto which are the "traumatic" stress field perturbations related to plate boundary processes in order to cause basin inversion and possibly other kinds of deformation of the interior of plates (e.g. Lithgow-Bertelloni and Guynn, 2004; Gosh et al., 2013; Schiffer and Nielsen, 2016).

The lithospheric density structure used to estimate GPE is derived from observations following the method of Nielsen et al. (2014) and Schiffer and Nielsen (2016), except that lithospheric density models are derived from palaeotectonic reconstructions through time, as in Peace et al. (2018a), rather than from the present only. The general approach is similar but not identical to that of Jones et al. (1996) and differs from that of Lithgow-Bertelloni and Guynn (2004) and Bird et al. (2008) by considering only lithospheric potential energy and radial tractions. Plate velocities, shear tractions and plate boundary forces are not considered.

The asthenosphere-lithosphere density column at each point is estimated as follows: The asthenosphere is defined by expansion of peridotite along a constant adiabatic gradient $[\partial T/\partial z] = 0.6$ °C/km with a potential temperature of 1315°C, a thermal expansion coefficient of $\alpha = 2.4 \cdot 10^{-5}$ K^{-1}, and a reference density of 3350 $kg \cdot m^3$. The temperature structure of the lithosphere and any overlying sedimentary layer are defined by a steady-state conductive geotherm using boundary conditions of 0°C at the surface and the corresponding adiabatic temperature at the respective lithosphere-asthenosphere boundary (LAB) depth. Representative values for thermal conductivities, radiogenic heat production rates and thermal expansion coefficients are assigned for the mantle lithosphere and the crustal and sedimentary layers; these are considered to be temperature-dependent (Schiffer and Nielsen, 2016). Sub-lithospheric mantle pressure anomalies (with reference to lithostatic pressure) and temperature anomalies (with reference to the used reference potential temperature) have also been applied to the model; these produce changes of the lithospheric geotherm and isostatic "dynamic topography".

Using a thin sheet approximation of the lithosphere (Bird and Piper, 1980; England and Houseman, 1986; England and McKenzie, 1982) and neglecting horizontal tractions at the base of the lithosphere, the equations of equilibrium of stresses are:

$$\begin{pmatrix} \frac{\partial \bar{\tau}_{xx}}{\partial x} + \frac{\partial \bar{\tau}_{xy}}{\partial y} = -\frac{1}{L}\left(\frac{\partial GPE}{\partial x} + L\frac{\partial \bar{\tau}_{zz}}{\partial x}\right) \\ \frac{\partial \bar{\tau}_{yx}}{\partial x} + \frac{\partial \bar{\tau}_{yy}}{\partial y} = -\frac{1}{L}\left(\frac{\partial GPE}{\partial y} + L\frac{\partial \bar{\tau}_{zz}}{\partial y}\right) \end{pmatrix}$$

where *x* and *y* are local horizontal coordinates, $\bar{\tau}_{xx}$,$\bar{\tau}_{yy}$,$\bar{\tau}_{xy}$ are the depth integrated horizontal deviatoric stresses, *L* is the reference depth, and $\bar{\tau}_{zz}$ is the vertical sub-lithospheric pressure anomaly. The final equations of the equilibrium of stresses, as defined in the above equation, are solved in 3D using the Finite Element Method (Zienkiewicz, 1977) in which the Earth's elastic shell is parameterised using a dense grid of flat, plane stress elastic triangles each with 15 degrees of freedom and with assigned elastic material parameters. Further methodological details are available in Schiffer and Nielsen (2016).

3.2 Model set up and parameterisation

The model parameterisation comprises the present lithospheric structure, including surface elevation, LAB depth, crustal and sedimentary layer thicknesses, corresponding densities, as well as sub-lithospheric pressure from Schiffer et al. (2018) and Schiffer and Nielsen (2016). Regarding the last of these, dynamic topography models from Müller et al. (2008) were expressed as sub-lithospheric pressure and temperature anomalies, with the assumption that they are constrained to the upper mantle. Positive sub-lithostatic pressure anomalies were defined to cause uplift of the lithospheric column, and vice versa. Additionally, the structural model was modified in the following ways. (1) The Greenland ice sheet was subtracted for any time steps older than 5 Ma. (2) Present-day dynamic topography from Schiffer and Nielsen (2016) was subtracted from the elevation model used for the reconstruction and, for each time-step, dynamic topography from Müller et al. (2008) was in turn added while allowing a maximum dynamic topography of 1000 m for these models. (3) The opening of previously non-existing and now subducted oceanic areas in the reconstructions were filled with oceanic lithosphere with ocean-age-dependent average values of surface heat flow, LAB depth, crustal thickness and topography observed in present-day oceanic lithosphere. (4) Sediments were subtracted from basins using smoothed sedimentation and subsidence rates observed in the North and Central Atlantic, as well as the Barents Sea (Anell et al., 2009; Berger and Jokat, 2008; Fiedler and Faleide, 1996; Gołędowski et al., 2012; Hjelstuen et al., 1996; Miller et al., 2005; Thiede et al., 1986; Wold, 1994; Wolf and Thiede, 1991). The subtracted sediments were then converted to a corresponding thickness of crystalline crust (scaling with the observed sedimentary and crustal densities) and added at the top of the crustal layer in the model.

Because these kinds of modifications can result in abrupt changes from cell to cell in the input grids in places, the models were smoothed by averaging the values within a running window of radius 50 km (topography and sedimentary layers), 100 km (upper and middle crust), 150 km (lower crust and Moho depth) and 200 km (LAB depth and surface heat flow) for each reconstructed time step. Since the analysis was conducted on a 1° × 1° grid, this mainly affects areas in high latitudes for shallower layers, but throughout the model for LAB depth. A linearised inversion method was used (e.g. Schiffer and Nielsen, 2016; Tarantola and Valette, 1982) that optimised the assigned free parameters (thickness, densities and heat production of the lithospheric layers, and thermal expansion of the mantle lithosphere) to fit palaeo-topography in a consistent isostatic model. The resulting lithospheric models are structurally consistent fitting topography, surface heat flow and lithospheric isostatic compensation (including a sub-lithospheric pressure anomaly that causes dynamic topography) within assigned representative a priori errors. The errors for topography and surface heat flow progressively increase for reconstructions back in time.

Reconstruction of the palaeotectonic lithosphere involves assumptions. For example, heat flow and thickness changes of the crust depend on the amount of material eroded or deposited and on thickening by orogenic processes. Except for regions of active mountain building (in the Alpine-Tethys belt) erosion rates are low and conservative estimates were made. The oceanic lithosphere in the models is governed by well-established cooling models. The models accordingly capture the essence of changes in the plate-scale GP stress field appropriate to this intraplate deformation study.

3.3 Results: 70 Ma, 40 Ma and 15 Ma GP palaeostress models

The three key time slices suggested by the compiled basin inversion data in section 2 are (1) Late Cretaceous-Palaeocene, (2) Eocene-Oligocene and (3) Miocene (cf. subsection 2.6). For the purposes of display of intraplate deformation in Figure 9 as well for the computation of palaeostress models, these are approximated to be at geological times 70 Ma, 40 Ma and 15 Ma, respectively. The main input grids representative of the lithospheric structure for these three reconstruction times (as well as, for comparison, the present day) are shown in Figure 10 and the computed GP palaeostress fields are seen in Figure 11.

The GP palaeostress fields seen in Figure 11 are presented in terms of principal horizontal stresses, which are the vertically averaged principal stresses relative to the lithostatic stress state (where stresses, equal in any direction at any depth, are simply the weight of the overburden). The trajectories of the respective computed principal palaeostress fields (Fig. 11) are also seen in the panels of Figure 10 (except for topography, row A), which provides some elucidation of the relative effects of the various contributing factors to the total (i.e., lithosphere thickness variations, crustal

thickness variations, sedimentary layer thickness variations, and sub-lithospheric mantle dynamics; rows B-E, respectively) and illustrates the relationship between the net geopotential energy derived from these and, in turn, the stress field derived from the net geopotential energy (row F).

The lithospheric structural elements for the palaeotectonic maps seen in Figure 11 were derived using GPlates (version 2.0) with the global reconstructions of Seton et al. (2012). Associated tectonic forces (N/m) can be estimated by multiplying the stresses by 100 km, the thickness of the elastic shell in the model. The contoured values (red-blue colour bar) are the magnitude of the maximum shear stress, which is the difference between maximum (most compressional) and minimum (least compressional or most tensional) of the principal horizontal stress components. It represents a measure of how likely faulting (or, more generally, failure) is (e.g. Ranalli, 1995). The actual numerical values can be judged relative to one another, but absolute values are not very meaningful given the simplifications of the simple structural/rheological model itself.

4. Distribution of intraplate deformation compared to palaeotectonic reconstructions and computed palaeostress fields

The schematic representations of intraplate deformation mined from the literature in section 2 and presented in Figures 9 have been superimposed on the GP palaeostress models in Figures 11. The detailed information that was mined, mainly from exploration-driven seismic profiling (section 2), were generalised to provide a more conceptual – but, nevertheless, observation-based – image of the temporal and spatial distribution of intraplate deformation in the study realm. This makes it more compatible with and more easily comparable to the intrinsically, regionally smooth character of the computed model GP palaeostress fields. All geographic place names and tectonic elements referred to in this section can be found in Figures 2.

First, a brief description of the modelled GP stress fields for each of the three key periods of tectonic transition in the North Atlantic-western Alpine-Tethys realm since the Late Cretaceous is provided. It is then considered how they compare with – and, indeed, how they contrast with – the distribution and structural trends of the compiled intraplate basin inversion structures. In respect of how the model GP stress fields role of reactivation of pre-existing structures, which is widely reported in the intraplate deformation literature, is assumed but is not within the scope of this section, which addresses the computed GP stress fields only in terms of observed intraplate deformation. Further discussion, including the role of inherited structures and heterogeneities, follows in section 5.

4.1 Computed stress fields

Figure 11 shows how the GP palaeostress regime in the study area (and adjacent tectonically active Alpine-Tethys belt) evolves from the Late Cretaceous to the Miocene. These can be broadly subdivided east and west into two main stress domains: (1) the East European Craton and its immediately surrounding terranes plus "Phanerozoic" Europe to its southwest across the Sorgenfrei-Tornquist-Tesseyre zone axis, this being the "fore-Alpine" platform north of the evolving and tectonically active Alpine-Tethys orogenic belt and (2) the northern North Atlantic realm, centred on Greenland, and evolving into having active seafloor spreading centres in the Cenozoic, first in the Labrador Sea-Baffin Bay corridor and later in what becomes the North Atlantic Ocean plus the southern North Atlantic realm to the south, adjacent to Phanerozoic Europe and actively accreting as a result of seafloor spreading during the whole of the period of the maps.

4.1.1 Eastern stress domain

The EEC sub-domain is characterised by large ambient (from all sides) principal compressional stresses orientated in a NE-SW direction throughout the entire Late Cretaceous-Cenozoic period. Both model principal stress magnitudes are large and, accordingly, the maximum shear stresses are small during this period. This is related to the thick lithosphere and crust of the EEC (cf. Figs. 10BC). This sub-domain represents the intrinsically stable part of the study area and its GP palaeostress regime, in terms of both principal stress relative magnitudes as well as maximum shear stresses, changes very little during the Late Cretaceous-Miocene time frame.

In the Phanerozoic sub-domain in west-central Europe where the lithosphere and crust are thinner, the NE-SW orientated principal stress is reduced compared to the EEC sub-domain and its orthogonal mate and, accordingly maximum shear stresses are higher. These display some variability with the greatest values to the northwest (modern Denmark area). As pointed out by Nielsen et al. (2014), this orientation of the GP stress field is consistent with the World Stress Map summary of present-day stress field in west-central Europe (Heidbach et al., 2016). The reduction of the NE-SW orientated principal stress component in this area is linked to the higher geopotential energy (Fig. 10F4) and, secondarily, the lower sub-lithospheric pressure anomalies (Fig. 10E4) and in this area compared to the EEC sub-domain. Since the stable EEC is to the north and west and the active orogenic belt is to the south throughout the Late Cretaceous-Cenozoic, the GP stress field of this sub-domain remains qualitatively similar throughout.

4.1.2 Western stress domain

The northern North Atlantic sub-domain is characterised by large differences in the two horizontal principal stresses, the most compressive of these generally orientated N-S or NW-SE and the other much less compressive or, often, extensional. The maximum shear stresses are, accordingly, much

larger in this domain. This is related to the thicker lithosphere and crust of Greenland lying between the thinner lithosphere and crust (with overlying sediments) of the Labrador Sea-Baffin Bay corridor and the proto-North Atlantic Ocean area, where pre-Late Cretaceous rifting has already thinned the lithosphere (cf. Figs. 10BCD). In the Late Cretaceous, maximum shear stress is also high in the Nares Strait region, between Ellesmere Island and Greenland, which records active strike-slip motion at this time.

The evolving sub-lithospheric pressure anomaly contribution to the GP palaeostress fields also plays a role (cf. Fig. 10E). The modelled GPE stress fields in this domain predict the geologically observed shift in extensional stresses from the Labrador Sea-Baffin Bay rift system to the northeast Atlantic Ocean. The former is characterised by extension and high maximum shear stress in the Late Cretaceous and Eocene (though more diffuse in the latter), which significantly diminish in the Miocene. The northeast Atlantic is characterised by extension and very high maximum shear stress after continental break-up throughout the Eocene-Oligocene to the Miocene, which is caused by the developing ridge push force.

Maximum shear stress in the central and southern northeast Atlantic is never markedly anomalous within the model realm because the domal mantle anomalies that produce ridge-perpendicular extension by ridge push also produce along-ridge extension.

4.2 Distribution of intraplate deformation compared to computed palaeostress fields

This section provides a brief description of how the modelled GP stress fields compare with the compiled intraplate basin inversion structures for each of the three key periods of tectonic transition in the North Atlantic-western Alpine-Tethys realm since the Late Cretaceous.

4.2.1 Late Cretaceous-Palaeocene

Figure 11a shows the computed Late Cretaceous (70 Ma) GP palaeostress with Late-Cretaceous-Palaeocene basin inversion features, as seen in Figure 9a, superimposed. Intraplate deformation is well-known, of course, at this time, having been amply documented by Ziegler (e.g. 1990) and other authors cited earlier. Previous work has broadly associated this period of intraplate deformation to early “Alpine-Tethyan” plate boundary interactions between the Laurasian (North American-Greenland-Eurasian) and African plate at this time and, indeed, inversion axes were dominantly NE-SW orientated in Europe in keeping with this.

The computed largest compressional GP principal stress direction in north-central Europe, the area that shows most intraplate deformation in the Late Cretaceous-Palaeocene is orientated NW-SE. This is perpendicular or highly oblique to the observed NE-SW orientated basin inversion. Outside

onshore Europe, the same is true for the North Sea and on the (proto-)Barents Sea margin. Inversion has been reported at one location between Great Britain and Greenland that is, in contrast, more compatible with the GP predicted stress field. With this exception, the geometry of the intraplate structures of this age seem more related to the EEC segment of the Laurasian plate, lying roughly concentrically to it rather than aligned with the complex, but roughly E-W orientated, Alpine deformation front. The locus of intraplate deformation at this time seems more related to strong gradients in the computed geopotential energy (GPE) of the study realm (Fig. 10F4), which is a more direct representation of the lithospheric-scale density structure rather than to the derived GP stress field itself. The inversion elements seen on Figure 11a that lie within the blue-coloured region of predicted low maximum shear stress are those of the TTZ and the Donbas Foldbelt (cf. Fig. 2b), the former corresponding to Palaeozoic and younger structures at the margins of the EEC and the latter with a Late Palaeozoic pericratonic rift basin. These structures also correspond with a changing geopotential energy field rather than a flat one (Fig. 10F4).

The model GP stresses in Figure 11a explicitly exclude horizontal plate boundary forces that may be exerted on the European fore-Alpine platform as a result of collisional effects (although temperature and pressure anomalies beneath this area and potentially linked to processes in the collisional belt are not). Accordingly, its misfit with the basin inversion trajectories implies superposition of additional forces generated by the Alpine-Tethys collision at this time to facilitate the intraplate deformation as has been widely recognised.

4.2.2 Eocene-Oligocene

Figure 11b shows that there is widespread occurrence of intraplate inversion structures of this age in the study realm. Compared to the Late Cretaceous-Palaeocene there is a strong shift from north-central Europe to the North Atlantic-Arctic realm (including Labrador Sea, Baffin Bay, Ellesmere Island, north Greenland, Barents Sea, Norwegian and the British-Irish continental margins) and in the Black Sea-Caucasus area as well as the periphery of the Alpine-Tethys collision zone (including along the Alpine Deformation Front from the Pyrenees to the Carpathians; cf. Fig. 2b). Much of north-central Europe does not display major basin inversion at this time although it is reported in some basins around the southern North Sea.

Inversion orientations in the Labrador Sea-Baffin Bay realm and in the periphery of the northern Greenland margin, from northern Baffin Bay to the west Barents Sea, are generally compatible to the GP maximum compression directions. These are readily correlated with Eurekan orogenesis, which drives – or feeds back – a fundamental plate reorganisation in this realm: rotation of Greenland prompted by the initial formation of the present North Atlantic plate boundary in the Palaeocene

leading to collision of Greenland and Ellesmere Island (and Svalbard) and cessation of further extension in the Labrador-Baffin corridor, completing the shift of the extensional regime to the North Atlantic. The relevant inversion structures include major, exposed, features defining the intraplate Eurekan Orogen itself from Axel Heiberg and Ellesmere islands in the west across northern Greenland to Svalbard in the east. Inversion extraneous to the Eurekan deformation belt include those in Baffin Bay, including the Ungava Fault Zone from Davis Strait to the northwest Labrador Sea, with one exception on the west Greenland margin, and – though more obliquely – the west Barents Sea. This is demonstrating that the plate boundary forces dominant at this time in this part of the study realm, which is no longer part of a contiguous Laurasian plate, are not collisional/subductional ones but only those generated at seafloor spreading plate boundaries. These contribute to the geopotential energy model of stresses, which, accordingly, fits with the observations. There is no subduction associated with the Eurekan Orogeny; it has occurred as intraplate deformation. Stresses arising at collisional plate boundaries, primarily associated with subducted slab negative buoyancy and convective processes associated with subduction, appear to be not relevant in this setting.

Elsewhere in the North Atlantic realm, inversion on the British-Irish margin is roughly compatible with the computed GP stress regime (within 45° of the least tensile principal stress), which may imply that it is driven by the intensifying North Atlantic ridge push effect. The effects of the Eurekan-aged North Atlantic spreading geometry reconfiguration are widely recognised (e.g. Gaina and Jakob, 2019). However, inversion on the Norwegian margin at this time is orthogonal to the most compressive stress axis, like much of the inversion recorded in west-central Europe in the Late Cretaceous-Palaeocene. The computed GP stress regime in both cases seems similarly to be dominated by the geopotential effects of the thick, cold lithosphere of cratonic and pericratonic Europe although it is noted that the shortening direction of inversion on the Norwegian margin at this time is also in keeping with the evolving ridge push nearby the craton edge.

Inversion in the Black Sea and Greater Caucasus Orogen is typically linked to Arabian-Eurasian collision that happened almost synchronously at this time. Typically, the GP stress orientations are not strongly compatible with the regional shortening directions. Eocene-Oligocene inversion elsewhere in the southeast of the study realm is even more proximal to the active deformation belt, with orientations also essentially incompatible with the GP stress field. This deformation, as for that in the fore-Alpine platform of west-central Europe in the Late Cretaceous-Palaeocene, can be considered to be predominantly driven by stresses derived from the nearby collisional/subductional plate interactions.

4.2.3 Miocene

Figure 11c shows that Miocene intraplate inversion structures are less well documented than earlier in the study realm and timing is less precise, although there are recognised reorganisations on the Alpine-Tethys plate boundary that have been linked to these in the eastern European-southern Eurasian part of the study realm, such as in the Black Sea.

Elsewhere, the documented basin inversion is limited to the Barents Shelf, the Norwegian margin and in the south of Ireland-Great Britain. The shortening directions associated with inversion at the first and last of these locations are not wholly incompatible with the computed GP stress fields. GP stresses on the Norwegian margin are highly oblique to the observations, in a framework very much like that described above in the Eocene-Oligocene, although Doré et al (2008) link it to compressional structures surrounding Iceland.

5. Discussion

The aims of this paper were to review and compile reported instances of intraplate inversion in the North Atlantic-western Tethys realm (Fig. 2) and then, by comparing the spatial and temporal distribution of these to age appropriate models of the geopotential (GP) palaeostress field, to make inferences regarding the cause and effect of intraplate stress and intraplate deformation. The following discussion of the results in the context of these aims is presented as follows. The first (sub-section 5.1) considers the imperfect relationship observed between intraplate deformation and predicted palaeostress derived from geopotential sources and, from this, proposes a concept of "traumatic stress" derived from geologically short-lived geodynamic processes at plate boundary interaction zones as being a diagnostic ingredient for generating periods of intraplate deformation in the North Atlantic-western Tethys realm. The second (sub-section 5.2) reviews the North Atlantic-western Tethys realm results and inferences about traumatic stress in the context of intraplate deformation on the contiguous North American and African plates, which share boundaries with the European plate. The last (sub-section 5.3) attempts to establish that traumatic stress within plates appears to be linked phenomenologically to rearrangements of spreading geometries between plates, which is inferred to imply a "top-down" framework for how plate tectonics is expressed at the Earth's surface.

5.1 Intraplate deformation and basin inversion: stress and rheology implications

5.1.1 "Traumatic stresses"

In any work that has considered the causal stress regime for intraplate deformation and basin inversion there is general agreement that compressional "far-field" stresses derived from nearby

plate boundaries are responsible. There is little in the way of quantitative assessment of this, it being generally a matter of temporal correlation of orogenic events at plate boundaries with active intraplate deformation rather than the proposal of any specific physical mechanism. Studies falling into this category include Ziegler (1987), Ziegler et al. (1995), Boldreel and Andersen, 1998; Blundell (2002), Marotta and Sabadini (2003), Scheck-Wenderoth and Lamarche (2005), Dyksterhuis and Müller (2008), Kley and Voigt (2008), Raimondo et al. (2014) and Dielforder et al (2019). The general idea is that stress propagation from the plate boundary into an intraplate setting implies that the lithosphere, at least within part of its thickness, is effectively elastic in its rheological response to plate boundary forces. This allows stresses to be propagated from the plate boundary to its interior "instantaneously" (e.g. Nielsen et al., 2007) where, given appropriately orientated pre-existing structures or thermo-mechanical heterogeneities (e.g. Hand and Sandiford, 1999; Sandiford and Quigley, 1999; Stephenson et al., 1999; Heron et al., 2019) these stresses may be large enough to cause failure in the lithosphere and permanent deformation such as basin inversion.

Nielsen et al. (2014) showed that the present-day ambient stress field where it is observed in west-central Europe (Heidbach et al., 2007) is similar to that predicted by a model of the present-day GP stress field, with the exception of several geodynamically complex areas. The correspondence of observed stress and modelled present-day GP stress notably fails in the vicinity of the active Alpine-Tethys plate boundary and there may be modifications, for example in Scandinavia, related to post-Pleistocene glacio-isostatic rebound. In any case, it was inferred that stresses associated with Alpine tectonics responsible for intraplate basin inversion in west-central Europe in the Late Cretaceous-Palaeocene were anomalous compared to those derived from stress-generating processes in the Alpine-Tethys convergence zone today. According to de Jager (2003), Late Cretaceous-Palaeocene basin inversion in west-central Europe is most strongly expressed in the Campanian, though it might have begun earlier during the Late Cretaceous. It terminated in the early Palaeocene (e.g. de Jager, 2003; Nielsen et al., 2007) coincident with a ~10 Myr break in the convergence of Africa and Europe (e.g. Rosenbaum et al., 2002), roughly synchronous with a time of continental collision that Ziegler (e.g. 1990) refers to as the Eo-Alpine phase of Alpine tectonics.

The southern, Tethyan, margin of Europe remains to this day a zone of general plate convergence and subduction, yet the European intraplate deformation structures seem to be tectonically dormant at this time (cf. Nielsen et al., 2014). This transient nature suggests that intraplate deformation only occurs when particular plate boundary processes are active, processes that are not taking place continuously along convergent plate boundaries. These plate boundary processes produce what are referred to here as "traumatic stresses", geologically short-lived, large magnitude stresses elastically transmitted into the plate interior, superimposed upon the background geopotential stress field,

689 then relaxed by the plastic deformation recorded in the geology, such as basin inversion. “Traumatic”
690 causative stresses must constructively interfere with the background GP stress field rather than
691 destructively, whether generating extensional or compressional deformation (the latter being on
692 primary interest in this paper). Coincidentally, though the importance of reactivation of pre-existing
693 structures for basin inversion and other intraplate deformation is widely recognised, it follows that
694 such inherited structures or weaknesses must also be favourably orientated with respect to the
695 composite stress field (trauma stresses plus GP stresses, not just the former).

696 The elastic stresses propagating from plate boundaries are relaxed at the location of the intraplate
697 deformation by a non-elastic response. This is most easily envisaged as faulting or shearing, either
698 newly formed (e.g. Stephenson et al. 2009) or as compressional reactivation of pre-existing faults
699 (e.g. Turner and Williams, 2004 and many others). Accordingly, the intraplate deformation occurs
700 only for as long as the governing stress field remains sufficient to drive it and these stresses are not
701 transmitted further into the interior of the plate. The non-elastic, permanent, deformation occurs as
702 long as the forces driving the process are renewed; the deformation remains once those driving
703 forces are removed from the plate boundary and the traumatic stresses are relaxed.

704 Any particular plate boundary process that produces “traumatic stress”, which is equivalent to saying
705 a “traumatic” or sudden change in the stress state of the plate, is not necessarily confined to the
706 convergent plate boundaries of a plate affected by intraplate deformation. This was demonstrated by
707 Nielsen et al. (2007) who showed Late Cretaceous-Palaeocene basin inversion in north-central
708 Europe was linked explicitly with the timing and style of plate break-up and new plate boundary
709 formation in the North Atlantic. High resolution age data from nannoplankton zones identified in a
710 research borehole in the Danish Basin (along the profile seen in Fig. 7a and located in Fig. 2a) allowed
711 Nielsen et al. (2007) to identify an initial stage of compressional shortening, involving reverse faulting
712 and uplift of a central structural high during a period of applied stress derived from the Alpine-Tethys
713 plate boundary, that ended abruptly at 62 Ma. While the renewing traumatic stress from the Alpine-
714 Tethys plate boundary was being relaxed as permanent intraplate deformation in north-central
715 Europe, other factors, including the traumatic stress field itself led to the break-up of the Greenland-
716 Eurasian plate in the North Atlantic. This rupture resulted in rapid changes in the sedimentary
717 architecture of depocentres associated with the intraplate deformation zone, which were shown to
718 be diagnostic of a sudden relaxation of elastic stresses transmitted from the Alpine-Tethys plate
719 boundary not by permanent *intraplate* deformation but, rather, by the birth of the incipient plate
720 boundary in the North Atlantic, namely permanent *interplate* deformation. This, in turn, terminated
721 the potential for renewal of traumatic stress in north-central Europe derived at the Alpine-Tethys
722 collisional plate boundary and, hence, the Late Cretaceous-Palaeocene inversion episode in this area.

The concept of “traumatic stress” does not necessarily mean that intraplate deformation cannot occur in its absence. What it does mean is simply that failure and deformation will occur in intraplate settings if the stress field is sufficiently high such that inherited structures are reactivated (or, possibly, new structures are formed if there are no existing “scars” appropriately orientated) – but with the understanding that the tectonic stress field itself comprises a GP background stress field (such as those modelled in this paper) plus a transient “traumatic” stress field, if and when it exists. Indeed, while the present study strongly suggests that such “trauma” must play a role in north-central European inversion structures active at various times since the Late Cretaceous, it also suggests that Eocene inversion in the Labrador Sea-Baffin Bay-Eurekan domain may have taken place in the absence of additional “trauma” since the inversion orientations are essentially compatible with those predicted by the computed GP stress field. The GP stress regime is itself primarily generated at plate boundaries in this realm, being the seafloor accretionary axes in Labrador Sea-Baffin Bay and, incipiently in the North Atlantic and Arctic. And, fortuitously, pre-existing structures (inherited in the Eurekan domain, for example, from Palaeozoic orogenesis; Piepjohn et al., 2016) are highly favourable to this.

5.1.2 Numerical modelling of intraplate basin inversion and role of rheology including structural inheritance

There are several published models of generic basin inversion (Nielsen and Hansen, 2000; Hansen and Nielsen, 2003; Sandiford, 1999; Sandiford et al., 2006; Buiter et al., 2009 and several others) aimed at linking specific tectonic boundary conditions to inversion of specific basins (e.g. Marotta and Sabadini, 2003; Nielsen et al., 2005; Sandiford et al., 2006; Nielsen et al., 2007; Stephenson et al., 2009). All of these pay substantial attention to rheological conditions, including the presence of weak zones, within the crust/lithosphere that may be favourable or unfavourable in specific settings.

Nielsen and Hansen (2000), Hansen and Nielsen (2003) and Buiter et al. (2009) emphasised the legacy heterogeneities and structures left in the lithosphere by previous rift basin formation and showed how these in general promoted and localised basin inversion in a subsequently compressional tectonic stress environment. Sandiford (1999) focused on the thermal changes in the lithosphere caused by rifting and sedimentary basin emplacement onto the attenuated lithosphere. Sandiford et al. (2006) explored the role of lower crustal rheology, in part proxied by depth to the Moho (as developed in Sandiford, 1999), and concluded that the strength contrast between lower crust and upper mantle could be an important factor in determining whether basins invert with a central uplift and outward-directed thrusting (e.g. Fig. 10) in contrast with basinward verging structures such as in Central Australia (e.g. Stephenson and Lambeck, 1985; Shaw et al., 1991).

Numerical modelling by Marotta and Sabadini (2003) affirmed that lateral rheological heterogeneities, again in part imposed by previous basin forming processes but also by the Palaeozoic suture between the East European Craton and younger terranes west of it that lies beneath the TTZ (Fig. 2), play an important role for intraplate deformation in Central Europe. Dyksterhuis and Müller (2008) also developed a theme emphasising complex lateral geometries in assembled continental lithosphere as being a kind of intraplate barometer to compression at plate margins, with application to southeastern Australia. Stephenson et al. (2009) showed that laterally heterogeneous thermal structure of the upper lithosphere caused by a thick sedimentary basin with lower bulk thermal conductivity than the surrounding igneous-metamorphic complex (specifically the Donbas Basin in southeastern Ukraine), can localise reverse shearing near the basin margin. Heron et al. (2015) demonstrated that mantle heterogeneity may "trump" crustal heterogeneity in continental lithosphere when investigating the Eocene-Oligocene inversion of the intraplate Eurekan Orogen and developed this further in Heron et al. (2016; 2019). Recently, in this regard, Bezada and Smale (2019) have argued that lithospheric mantle structure may be strongly involved in the localisation of intraplate seismicity based from studies of the attenuation of teleseismic earthquake phases. Carpentier et al. (2009) presented evidence from stochastic attributes of controlled-source deep seismic reflection profiling that suggests sub-crustal lithosphere structure beneath an old rift zone is more chaotic, hence potentially more attenuating to teleseismic waves, than away from the rift zone.

For all intents and purposes, all of this work consolidates the general consensus that where intraplate deformation occurs is largely predestined by inherited structure, which includes inherited compositional and thermal heterogeneities in the lithosphere (including variable crustal thickness) as well as actual faults and structurally weak zones (viz. Schiffer et al., 2019a). And, as mentioned at the outset, basins, and rift basins especially, "tick a number of boxes" in this regard.

There is indeed a preponderance of studies supporting the concept that intraplate deformation is intimately linked with inheritance and nothing from the currently compiled maps of basin inversion in the Alpine-Tethys-North Atlantic region strongly suggests otherwise. What the present compilation does show is that intraplate deformation, if reflecting reactivations of earlier structures such as in basin inversion, is not systematically orientated with respect to the geopotential induced stress field of the host lithosphere. The main inference, therefore, as discussed above, is confirmation that stresses derived from processes taking place at adjacent collisional/convergent plate boundaries are often required – but are not a prerequisite – for the occurrence of intraplate deformation. Further, these processes may be relatively short-lived geologically speaking so, in some manner, representing anomalous activities such as rupture and rift propagation/migration (e.g. Le Breton et al., 2012) or

789 subduction locking (e.g. Rosenbaum et al., 2002) or rearrangements linked with volcanism and back-
790 arc basin formation.

791 *5.2 Extraplate context of basin inversion in the North Atlantic-western Tethys realm*

792 As outlined above, the working hypothesis is that the superposition of collisional plate boundary
793 derived "traumatic" stress changes superimposed on the long-term, ambient quasi-steady state
794 geopotential stress field produces deformation of favourably orientated weak structures in
795 continental interiors. From studies of intraplate deformation beyond the North Atlantic-western
796 Tethys realm, it seems that the most often invoked sources of stress changes are those arising from
797 the occurrence of orogenies at plate margins and from changes in the spreading/subduction
798 configuration of the adjacent oceanic domain. Surface motion and intracontinental deformation
799 induced by mantle flow (e.g. Finzel et al., 2015) may also be relevant. This section provides a brief
800 overview of contemporaneous intraplate effects in the plates contiguous to the North Atlantic-
801 western Tethys study realm.

802 *5.2.1 North America*

803 Present-day seismicity highlights present-day intraplate deformation zones in the continental North
804 American plate. One such is the New Madrid Seismic Zone in the United States (e.g. Tuttle et al.,
805 2002), where faults formed during rift formation in a Neoproterozoic-Cambrian extensional stress
806 regime are probably being reactivated at present in a (trans)compressional stress regime (cf. Mooney
807 et al., 1983; Levandowski et al., 2018). Possibly the New Madrid structure will provide an excellent of
808 intraplate basin inversion were it to be revisited in 50 My time. Nevertheless, the plate-scale
809 character of the present-day observed stress field (e.g. Heidbach et al., 2007; 2018; Levandowski et
810 al., 2018) appears to be dominated by geopotential stresses (e.g. section 3) though obviously
811 includes any current plate boundary sourced stress as well. It is also roughly compatible with the
812 observed earthquake focal mechanisms although local contributions to geopotential stresses,
813 including inherited ancient basement structures producing lithospheric density contrasts
814 (Levandowski et al., 2016), may be important for localising seismicity and perhaps are even sufficient
815 for inducing it. For example, Murphy et al. (2019) recently ascribed seismicity in the southeastern
816 United States (e.g. the 2011 Virginia earthquake) to be largely explicable by forces arising from
817 crustal thickness variations in the region. Anomalous temperature within the lithosphere possibly
818 also plays a role (Liu and Zoback, 1997) and a minor perturbation in the regional stress field indicated
819 by earthquake focal mechanisms in the vicinity of the New Madrid area has been modelled by
820 Levandowski et al. (2016) as evidence of the refractive effects of dense and more rigid material in the
821 lower crust, possibly inherited from the earlier rifting episode (Ervin and McGinnis, 1975).

This is all generally compatible with the premise that the intraplate stress field is dominantly the geopotential stress field away from plate boundaries but that smaller scale heterogeneities in crustal structure (smaller than those considered here) may be very important in localising intraplate seismicity and, hence, deformation. Whether this can occur in the absence of traumatic tectonic stresses, which have been inferred to exist from the geological record (but not the neotectonic one), is unclear since present-day traumatic stress cannot be differentiated from the observed stress field, but it seems plausible given the ubiquitous role of inheritance in all studies of past/present intraplate deformation/seismicity.

Looking at the history of the North American continental plate, van der Pluijm et al. (1997), using twinned calcite in carbonate rocks in front of the Sevier and Appalachian orogenies (western and eastern North America, respectively), inferred an exponential decay of differential palaeostress of approximate decay length 200 km with distance perpendicular to the relevant orogenic front. This is order of magnitude comparable to the model of England et al. (1985), based on viscous thin sheet theory, for an indenter wavelength of approximately 2000 km. In spite of the significant differences between the thin-skinned, Late Mesozoic Sevier orogeny and the continent-continent collision of the Late Palaeozoic Appalachian orogeny with crustal involvement they found that the differential stress distributions were very similar and far reaching. The similarity suggests that continental interior stresses are largely insensitive to the details of the stress generating source region meaning that far-field stress transmission does not contain information about the structural details of the source. In any case, twinned calcite as a palaeopiezometer should be used with caution (e.g. Rybacki et al., 2013).

Macro-structural evidence, such as used in the present study, may be more robust. In North America Pinet (2016) used tectonic arguments of reactivation of normal faults to argue for the influence of the far field stress effects of the Appalachian orogenesis in the Hudson Bay region more than 1400 km away from the orogenic front. Marshak et al. (2000) suggested that intracratonic deformation associated with Laramide and ancestral Rockies tectonics in western North America, generally utilised favourably orientated weak basement structures in the upper crust, which were inherited from Proterozoic rifting events between 1.3 and 1.1 Ga and 0.9 and 0.7 Ga. Reactivation of the structures then occurred during Phanerozoic compressional orogenies. This extreme case of utilisation of structural inheritance across eons emphasizes the potential importance of structural history to the understanding of intra continental deformations (cf. Schiffer et al., 2019b, for the North Atlantic realm).

5.2.2 Africa

The African plate has been coupled to Europe during the closure of Tethys since the Santonian at approximately 84 Ma. In the middle to eastern Mediterranean, subducting ocean lithosphere still separates the European and African continents, and the Alpine-Tethys zone generally remains a zone of tectonic convergence. This region provides an example of the variability of stress transmission from the source region of the continental margin into the continental interior, not only in Europe, as forms an important foundation of the present paper, but of Africa.

Guiraud and Bosworth (1999) found that the inversion-related features in North Africa were uneven in intensity and distribution, but usually utilised existing rifts (as, generally, in Europe, documented in section 2 of this paper). Later, Bosworth et al. (2008) suggested that the irregular shape of the North African continental margin accounts for the most severe shortening being found in the protruding region of Cyrenaica in Libya whilst its deformation provided a regional stress shadow that protected areas south and southeast (the Sirte Basin and the far Western Desert of Egypt) from compressional shortening. The eastern region of the Western Desert and Sinai, were not, however, shielded by the stress-consuming Cyrenaica inversion, and recorded strong contemporaneous compressional deformation (Syrian arc inversion structures; e.g. Moustafa, 2013). This exemplifies how the detailed tectonic evolution of individual intra continental basins can depend on their positions in relation to the stress generating orogenic processes at the continental margin and highlights the absolute importance of inheritance. The formation of these inversion structures took place at the same time as the Late Cretaceous-Palaeocene inversion structures of the North Atlantic-western Tethys realm (i.e., section 4.2.1).

The West and Central African Rift System (WCARS) fingers between the three northern cratonic blocks of Africa, and the individual branches have been in favourable positions for reactivation during plate-wide stress changes (e.g. Guiraud et al., 1992; Guiraud, 1993). A recent paper (El Hassan, et al. 2017) presents detailed documentation of Late Cretaceous inversion in in the WCARS from exploration seismic data. Janssen et al. (1995) compared published correlation charts of stratigraphic events with tectonic subsidence rates of fourteen basins on African margins and in intracontinental rifts with the break-up history of Gondwana and found a strong correlation between changes in plate motions and reactivation of extensional basins in the African plate. The compilation of Guiraud and Bosworth (1997) of Senonian (89-65 Ma) tectonic events across Africa and Arabia demonstrated a strong correlation between a shift in opening directions of the Atlantic oceanic spreading system and the occurrence of regional intraplate compressional deformations. In particular, the onset of Africa's counter clockwise rotation towards Europe in the Santonian at ca. 84 Ma was registered by evidence for compression throughout Africa.

Fairhead et al. (2013) found a strong correlation between changes in basin development, including the development of unconformities, and changes in oceanic plate motions, similarly to Janssen et al. (1995). They suggested a causative relationship between this correlation with unconformities on the continental margins of Africa and South America but did not pay direct attention to intraplate compressional deformation. It was speculated that the causative mechanism for these unconformities could be the flexural response of the lithosphere to changes in its in-plane state of stress along the lines proposed by Cloetingh (1986) and Braun and Beaumont (1989). Fairhead et al. (2013) specifically noted the short-term nature of such stress changes so providing indirect support to the concept of traumatic stresses being associated with oceanic spreading centre reorientations and, possibly, the effects of these on the contiguous Africa-Europe collisional plate boundary.

5.3 Intraplate deformation and "top down" plate tectonics

Reorganisation of ocean spreading has been invoked as an explanation for intracontinental stress changes by the firm grip that oceanic lithosphere holds on the continents. For example, Faure et al. (1996) attributed the stress regimes inferred in the Quebec-New England igneous province to the Early Cretaceous rifting between Labrador and Greenland. They surmised that variations of spreading rate and plate boundary conditions of North America in the Late Cretaceous-Palaeocene led to stress inversion in eastern North America and the compressional stress field that is still present today. Recently, Gaina and Jakob (2018) invoked changes in seafloor spreading rates in the North Atlantic, Arctic and northeast Pacific oceans in the 60-35 Ma time interval as a possible explanation for "global Eocene tectonic unrest". Carminati et al (2009) proposed a possible link between shifts in the Mid-Atlantic Ridge seafloor spreading axis and Cenozoic intraplate effects in the North Atlantic as a result of possible mantle dynamics effects of the former.

Australia separated from the Madagascar/Indian block and later from Antarctica and became surrounded by spreading and aging ocean floor and, not surprisingly, the evolution of the oceanic plates surrounding the Australian continent has been invoked as a source of stress changes in the plate interior. Cathro et al. (2006) interpreted the Cretaceous and Miocene inversion in the Dampier sub-basin, northwest Australia, to be a consequence of a major plate reorganisation related to the northward movement of India and the commencing break-up between Australia and Antarctica. Hengesh and Whitney (2016) saw transcurrent reactivation of Australia's western passive margin and interpreted this as an example of intraplate deformation from the central Indo-Australian plate. Dyksterhuis and Müller (2018) studying the last 100 Myr of stress evolution in the Australian plate found that forces at plate margins can be transmitted over thousands of kilometres into continental interiors, in accord with the conclusions of many authors, including Rajabi et al. (2017) who found

921 that local structure causing perturbations in the stress field may be more significant than previously
922 realised, particularly in eastern Australian basins. Nearby, in the Tasman Sea area off eastern
923 Australia, Sutherland et al. (2017) demonstrate that the onset of subduction in the western Pacific
924 (e.g. Tonga-Kermadec) correlates with a period of what is essentially intraplate deformation taking
925 place during the Eocene in continental but also oceanic lithosphere.

926 Recently, Brune et al. (2016) carried out a quasi-global survey of rift kinematics and, on this basis,
927 proposed a dynamic mechanism involving non-linear feedback between rift forces and resistive
928 forces to explain "rapid absolute plate motion changes". Although Brune et al. (2016) did not include
929 the North Atlantic margins in their study, it is notable that the two Late Cretaceous and younger
930 periods of rapid plate motion changes they infer are Late Cretaceous-Palaeocene (from the Australia-
931 Antarctica margins) and Late Eocene-Oligocene (from the South China Sea), which correspond to two
932 of the periods highlighted by the present study of intraplate deformation in the North Atlantic-Tethys
933 realm. Further, Gaina and Jakob (2018) modelled global oceanic lithosphere age and spreading rates
934 for approximately the same period (60 to 35 Ma interval), focusing on the North Atlantic, Arctic and
935 NE Pacific oceans, and identified the Eocene generally as a time of "global tectonic unrest". Specific
936 to the North Atlantic-Tethys realm, Le Breton et al. (2012) found, on the basis of a new plate
937 kinematic restoration, that both the Eocene-Oligocene and Miocene intraplate deformation phases
938 highlighted by the present study correspond to times of left-lateral strike slip on the Faeroe Fracture
939 Zone (Eocene-Oligocene) and the Jan Mayen Fracture Zone (Eocene-Oligocene and Miocene) and
940 development of inversion structures in adjacent regions. Oceanic fracture zones may be, in general,
941 sensitive markers of "traumatic" intraplate stresses given their sensitivity to changes in plate
942 kinematics (e.g. Phethean et al., 2016; Schiffer et al., 2018).

943 From a distinctly different point of view, one of stratigraphy and lithofacies, Embry et al. (2018),
944 having identified more than fifty large-magnitude tectonically induced sequence boundaries in seven
945 Phanerozoic sedimentary basins of the Canadian High Arctic, proposed that they were the product of
946 plate tectonic reorganisations that changed the speed and direction of plate movements. Each
947 episode would have begun with uplift and regression of the basin margin, followed by rapid
948 subsidence and transgressive flooding (hence, T-R sequences). According to flexural models
949 responding to "traumatic" stresses generating at plate boundaries (e.g., Nielsen et al., 2007) this
950 would correspond to enhanced tectonic compression (or reduced extension) followed by extension
951 (or reduced compression). However, the strength of correlations across ocean spreading ridges or
952 even over a few hundred kilometres on the same continental margin or between individual margins
953 of rifts is tempered when considering the possible stratigraphy generating potential of sub-
954 lithospheric small-scale convection. Petersen et al. (2010), for example, showed that T-R sequences

with periodicities in the range 5-20 Myr can be produced in this way, which compares with the periodicity of 10 Myr identified by Embry et al. (2018). These predominantly vertical displacements, of moderate amplitude, do not constitute "basin inversion" as used in this study.

All of these kinds of observations and considerations inexorably link intraplate deformation with what can be considered geologically rapid – and, hence, "traumatic" – changes in contiguous plate boundary configurations and, accordingly, the processes taking place there. Changing kinematics on the boundary between two plates (and, hence, changing "boundary conditions" on related geodynamic processes occurring there) feeds back to contiguous plate boundaries on both plates, and so on. Such plate reorganisations occur on timescales of 10-20 Myr or less and the stresses caused by them, propagated elastically to the interiors of contiguous plates are superimposed on the more slowly changing, inherent GP lithospheric stress fields and are relaxed by permanent intraplate deformation when inheritance is favourably disposed to this superposition. All evidence that has been contemplated pertaining to intraplate deformation seems to suggest that its very existence and its spatial and temporal distribution in the geological past is compatible with a "plate" theory of tectonics and that it offers little that can be placed in a "plume" theory of tectonics (cf. Foulger et al., 2005).

6. Summary and conclusions

A compilation of intraplate deformation structures, mainly as expressed as sedimentary basin inversion structures, formed since the Late Cretaceous in the North Atlantic-western Alpine-Tethys realm has been generalised and compared to palaeostress fields computed from geopotential (GP) energy gradients for three key periods of tectonic transition and intraplate deformation in the study realm, these being Late Cretaceous-Palaeocene, Eocene-Oligocene and Miocene. The results have been discussed in the context of a broad literature review with the aim of illuminating the causes and effects of intraplate tectonics at the plate scale and at a global tectonic scale. Conclusions in this regard clearly build upon the pioneering work of Ziegler and others when documenting European intraplate inversion in the 1980s and considering its implications for tectonic driving mechanisms, the main added value here being two-fold: (i) the quantitative aspect of the present study, which incorporates models of GP palaeostress at times of intraplate deformation and (ii) the stronger focus on Cenozoic intraplate deformation, not just in continental Europe but throughout the North Atlantic, this also benefitting from better constraints on the timing of deformation of key features such as the intraplate Eurekan and Crimean-Caucasus orogens.

What follows is a short summary of the regional tectonic evolution of the study realm and its expression as intraplate deformation and palaeostress regimes for the three identified key periods of tectonic transition. Finally, a series of more generic conclusions regarding the geodynamics of intraplate deformation based on the results and discussion is presented.

6.1 Tectonic setting, intraplate stresses and basin inversion: summary

(1) Late Cretaceous-Palaeocene:

- Computed Late Cretaceous-Palaeocene principal horizontal stress directions are generally incompatible with the (smoothed) orientations of basin inversion structures (neglecting any role of inheritance or other locally derived perturbation) in west-central Europe. The widely-recognised implication is that an additional NW-SE orientated force derived from the Alpine-Tethys collisional plate boundary was involved in generating basin inversion at this time in west-central Europe.
- Adria-Europe collision occurs ("Eo-Alpine" phase of Alpine Orogeny) and an unknown geodynamic process associated with the collisional/subductional plate boundary at this time produces the requisite "traumatic" intraplate compressional stresses linked to regionwide tectonic inversion in Central Europe.
- The build-up and culmination of this "traumatic" event are interconnected with seafloor spreading kinematics in the central Atlantic Ocean, which record a period of very low or no Europe-Africa plate convergence in the latest Cretaceous-Palaeocene. This, in turn, leads to the onset of the break-up of Laurasia in the present-day North Atlantic Ocean with Greenland being detached from the Eurasian plate in the Palaeocene. This event terminates the renewal of traumatic stresses and leads to the cessation of the Late Cretaceous-Palaeocene phase of intraplate deformation in west-central Europe.
- The geologically sudden rupturing of Laurasia in the proto-North Atlantic can itself be considered a rapid plate boundary reconfiguration leading to a "traumatic" change in the stress fields of the contiguous plates. It promotes an acceleration of extension in the northern Labrador Sea-Baffin Bay leading to seafloor spreading in the latter.

(2) Eocene-Oligocene:

- There is a notable shift of locus of basin inversion from central-northern Europe in the Late Cretaceous-Palaeocene to the North Atlantic-Arctic realm and to the periphery of the Alpine collision after the onset of North Atlantic break-up in the Eocene. In the former, this is accompanied by a significant change in the computed GP stress field around Greenland, with

large extensional stresses in the Labrador Sea-Baffin Bay corridor decreasing and initially weaker extension in the North Atlantic increasing.

- Greenland acts as an independent plate and rotates, causing extensive basin inversion on its northern (Ellesmere Island-Svalbard) and western (Baffin Bay) margins, including the formation of the intraplate Eurekan Orogen, which can be considered as a case of profound basin inversion (deforming and uplifting sedimentary strata deposited in this area after Palaeozoic orogenesis). The concurrent GP stress state is compatible with basin inversion in this realm at this time. This state of stress is a direct consequence of trauma in the Laurasian plate that led to North Atlantic break-up but is not itself overprinted by concurrent "traumatic stresses" as defined in this work.
- Northern Atlantic margins display local basin inversion promoted by the emerging North Atlantic ridge push, which is part of the evolving GP stress field in this area.
- Basin inversion still occurs immediately along the periphery of the Alpine-Tethys belt, most obviously linked with the nearby collision of the Eurasian plate with the Arabian plate (e.g. Crimea-Greater Caucasus intraplate orogen), but is mostly absent in west-central Europe, the traumatic stress field being generated at the Adria-Europe plate boundary having been relaxed and no longer renewed after the Palaeocene.

(3) Miocene:

- Seafloor spreading has ended in the Labrador Sea-Baffin Bay corridor and Greenland is now solidly part of the North American plate. All basin inversion processes surrounding the former "Greenland plate" have terminated.
- Basin inversion continues on the Norwegian margin and in the Barents Sea, as well as south of Ireland and Great Britain, likely linked to NE Atlantic ridge push and possibly developments related to the emerging Eurasia Basin of the Arctic Ocean.
- Miocene inversion occurs in southeastern Europe in the Black Sea and its margins but has not been recorded since, although there is active (transpressional) seismicity along the northern margin of the Black Sea.

6.2 The geodynamics of intraplate deformation: general conclusions

(1) Intraplate lithosphere stresses are those dominantly being generated by plate scale geopotential energy effects rather than collisional plate boundary effects and these can be considered to comprise the "background" intraplate stress field.

(2) Intraplate deformation, such as basin inversion, occurs – it goes without saying – whenever stress exceeds strength causing recordable permanent deformation at a suitable locus within the

lithosphere. This can be dependent upon geologically rapid changes at plate boundaries (short compared to the lifespan of plate boundary zones themselves) that produce an additional "traumatic" component of intraplate stress.

(3) Intraplate deformation is promoted if/when the "traumatic" stresses constructively interfere with those derived from the background geopotential energy gradients and, further, the resulting causative, net stress field is favourably orientated with respect to pre-existing structures or other heterogeneities embedded within the lithosphere.

(4) "Traumatic" stresses are mainly an elastic response to the governing plate boundary processes, requiring that intraplate continental lithosphere is strong, with rigid-elastic properties, but that its elastic strength is finite and can fail to produce permanent plastic deformation in the presence of a favourably orientated net stress field.

(5) That intraplate deformation expressed as sedimentary basin inversion occurs in a stress field related to lithosphere potential energy variations modified by tectonic forces produced at plate boundaries, means that it is a "top-down" ("plate" model rather than "plume" model) tectonic phenomenon.

Acknowledgments

The authors wish to acknowledge the feedback of two anonymous reviewers, whose comments and suggestions have led to a substantially improved manuscript. CS's (now at Uppsala University, Sweden) postdoctoral fellowship at Durham University was financed by the Carlsberg Foundation. AP's (now at McMaster University, Canada) postdoctoral fellowship at Memorial University of Newfoundland was funded by the Hibernia project geophysics support fund. SJ's postdoctoral fellowship at the University of Calgary is funded by Natural Sciences and Engineering Research Council of Canada.

References

Andersen, M.S., Nielsen, T., Sørensen, A.B., Boldreel, L.O., Kuijpers, A., 2000. Cenozoic sediment distribution and tectonic movements in the Faroe region. Global and Planetary Change, 24, 239-259.

Anell, I., Thybo, H., Artemieva, I.M., 2009. Cenozoic uplift and subsidence in the North Atlantic region: Geological evidence revisited. Tectonophysics, 474, 78-105. doi:10.1016/j.tecto.2009.04.006

Artyushkov, E.V., 1973. Stresses in the lithosphere caused by crustal thickness inhomogeneities. Journal of Geophysical Research, 78, 7675-7708.

Banerjee, P., Bürgmann, R., Nagarajan, B., Apel, E., 2008. Intraplate deformation of the Indian subcontinent. Geophysical Research Letters, 35, L18301. doi:10.1029/2008GL035468

Berger, D., Jokat, W., 2008. A seismic study along the East Greenland margin from 72 N to 77 N. Geophysical Journal International, 174, 733-748.

Bezada, M.J., Smale, J., 2019. Lateral variations in lithospheric mantle structure control the location of intracontinental seismicity in Australia. Geophysical Research Letters. doi:10.1029/2019GL084848

Bird. P., Liu, Z., Rucker, W.K., 2008. Stresses that drive the plates from below: definitions, computational path, model optimization, and error analysis. Journal of Geophysical Research: Solid Earth, 113 (B11).

Bird, P., Piper, K., 1980. Plane-stress finite-element models of tectonic flow in southern California. Physics of the Earth and Planetary Interiors, 21, 158-175. doi:10.1016/0031-9201(80)90067-9

Bjørnestad, 2012. Structural analysis of the Leirdjupet Fault Complex in the southwestern Barents Sea, Master's Thesis, Department of Geosciences, University of Oslo.

Blaich, O.A., Tsikalas, F., Faleide, J.I., 2017. New Insights into the tectono-stratigraphic evolution of the southern Stappen High and its transition to Bjärnäya Basin, SW Barents Sea. Marine and Petroleum Geology, 85, 89-105. doi:10.1016/j.marpetgeo.2017.04.015

Blundell, D.J., 2002, Cenozoic inversion and uplift of southern Britain: Geological Society, London, Special Publications, 196, 85-101.

Boldreel, L.O., Andersen, M.S., 1993. Late Palaeocene to Miocene compression in the Faeroe-Rockall area. Geological Society, London, Petroleum Geology Conference series, 4, 1025-1034.

Boldreel L.O., Andersen, M.S., 1998. Tertiary compressional structures on the Faroe-Rockall Plateau in relation to northeast Atlantic ridge-push and Alpine foreland stress, Tectonophysics, 300, 13-28.

Bosworth, William, Ahmed S. El-Hawat, Daniel E. Helgeson, Kevin Burke, 2008. Cyrenaican "shock absorber" and associated inversion strain shadow in the collision zone of northeast Africa. Geology, 36, 695-698. doi:10.1130/G24909A.1

Braathen, A., Bergh, S.G., 1995. Kinematics of Tertiary deformation in the basement-involved fold-thrust complex, western Nordenskild Land, Svalbard: tectonic implications based on fault-slip data analysis, Tectonophysics, 249, 1-29.

1111 Braun, J., Beaumont, C., 1989. A physical explanation of the relationship between flank uplifts and
1112 the break-up unconformity at rifted continental margins. Geology, 17, 760-764.

1113 Breivik, A.J., Faleide, J.I., Gudlaugsson, S.T., 1998. Southwestern Barents Sea margin: late Mesozoic
1114 sedimentary basins and crustal extension. Tectonophysics, 293, 21-44.

1115 Brekke, H., Riis, F., 1987. Tectonics and basin evolution of the Norwegian shelf between 62°N and
1116 72°N, Norsk Geologisk Tidskrift, 67, 295-321.

1117 Brune, S., Williams, S.E., Butterworth, N.P., Müller, R.D., 2016. Abrupt plate accelerations shape
1118 rifted continental margins. Nature, 536, 201-204. doi:10.1038/nature18319

1119 Buiter, S.J.H., Pfiffner, O.A., Beaumont, C., 2009. Inversion of extensional sedimentary basins: a
1120 numerical evaluation of the localisation of shortening. Earth and Planetary Science Letters, 288, 492-
1121 504. doi:10.1016/j.epsl.2009.10.011

1122 Calais, E., Camelbeeck, T., Stein, S., Liu, M., Craig, T.J., 2016. A new paradigm for large earthquakes in
1123 stable continental plate interiors. Geophysical Research Letters, 43, 10,621-10,637.
1124 doi:10.1002/2016GL070815

1125 Carminati, E., Cuffaro, M., Doglioni, C., 2009. Cenozoic uplift of Europe. Tectonics, 28, TC4016.
1126 doi:10.1029/2009TC002472

1127 Carpentier, S., Roy-Chowdhury, K., Stephenson, R.A., Stovba, S.M., 2009. Delineating tectonic units
1128 beneath the Donbas Foldbelt by using scale lengths estimated from DOBRE 2000/2001 deep
1129 reflection data. Journal of Geophysical Research, 114, B10315. doi:10.1029/2008JB006124, 2009

1130 Cathro, D.L., Karner, G.D., 2006. Cretaceous-Tertiary inversion history of the Dampier Sub-basin,
1131 northwest Australia: Insights from quantitative basin modelling. Marine and Petroleum Geology, 23,
1132 503-526.

1133 Chalot-Prat, F., Doglioni, C., Falloon, T., 2017. Westward migration of oceanic ridges and related
1134 asymmetric upper mantle differentiation. Lithos, 268-271, 163-173. doi:10.1016/j.lithos.2016.10.036

1135 Chauvet, F., Geoffroy, L., Guillou, H., Maury, R.C., Le Gall, B., Agranier, A., Viana, A., 2019. Eocene
1136 continental breakup in Baffin Bay. Tectonophysics, 757, 170-186.

1137 Chesher, J.A., 1991. Geology of the United Kingdom, Ireland and the adjacent continental shelf
1138 (south sheet): British Geological Survey, 1 sheet, scale 1:1 000 000.

1139 Clausen, O.R., Nielsen, O.B., Huuse, M., Michelsen, O. 2000. Geological indications for Palaeogene
1140 uplift in the eastern North Sea Basin. Global and Planetary Change, 175-187.

1141 Cloetingh, S., 1986. Intraplate stresses: A new mechanism for fluctuations of relative sea level.
1142 Geology, 14, 617-620. doi:10.1130/0091-7613

1143 Coblentz, D.D., Richardson, R.M., Sandiford, M. 1994. On the gravitational potential of the Earth's
1144 lithosphere. Tectonics, 13, 929-945.

1145 Dadlez, R., Narkiewicz, M., Stephenson, R.A., Visser, M., van Wees, J-D. 1995. Tectonic evolution of
1146 the Polish Trough: modelling implications and significance for central European geology.
1147 Tectonophysics, 252, 179-195.

1148 de Jager, J., 2003. Inverted basins in the Netherlands, similarities and differences. Netherlands
1149 Journal of Geosciences (Geologie en Mijnbouw), 82, 355-366.

1150 de Lugt, I.R., van Wees, J.D., Wong, T., 2003. The tectonic evolution of the southern Dutch North Sea
1151 during the Paleogene: basin inversion in distinct pulses. Tectonophysics, 373, 1, 141-159.
1152 doi:10.1016/S0040-1951(03)00284-1.

1153 Dielforder, A., Frasca, G., Brune, S., Mary Ford, M., 2019. Formation of the Iberian-European
1154 convergent plate boundary fault and its effect on intraplate deformation in central Europe.
1155 Geochemistry, Geophysics, Geosystems, 20, 2395-2417. doi:10.1029/2018GC007840

1156 Doglioni, C., Panza, G., 2015. Polarized Plate Tectonics. Advances in Geophysics, 56, 1-167.
1157 doi:10.1016/bs.agph.2014.12.001

1158 Doré, A.G., Lundin, E.R., 1996. Cenozoic compressional structures on the NE Atlantic margin: nature,
1159 origin and potential significance for hydrocarbon exploration. Petroleum Geoscience, 2, 299-311.
1160 doi:10.1144/petgeo.2.4.299

1161 Doré, A.G., Lundin, E.R., Fichler, C., Olesen, O., 1997. Patterns of basement structure and reactivation
1162 along the NE Atlantic margin: Journal of the Geological Society, 154, 85-92.
1163 doi:10.1144/gsjgs.154.1.0085.

1164 Doré, A.G., Lundin, E.R., Kusznir, N.J., Pascal, C., 2008. Potential mechanisms for the genesis of
1165 Cenozoic domal structures on the NE Atlantic margin: pros, cons and some new ideas. Geological
1166 Society, London, Special Publications, 306, 1-26.

1167 Døssing, A., Hopper, J.R., Olesen, A.V., Rasmussen, T.M., Halpenny, J. 2013. New aero-gravity results
1168 from the Arctic Ocean: linking the latest Cretaceous-early Cenozoic plate kinematics of the North
1169 Atlantic and Arctic Ocean, Geochemistry, Geophysics, Geosystems, 14, 4044-4065.
1170 doi:10.1002/ggge.20253

1171 Dyksterhuis, S., Muller, R.D., 2008. Cause and evolution of intraplate orogeny in Australia. Geology,
1172 36, 495-498, doi:10.1130/G24536A.1

1173 El Hassan, W.M., Farwa, A.G., Awad, M.Z., 2017. Inversion tectonics in Central Africa Rift System:
1174 Evidence from the Heglig Field. Marine and Petroleum Geology, 80, 293-306.

1175 Embry, A., Beauchamp, B., Dewing, K., Dixon, J., 2018. Episodic tectonics in the Phanerozoic
1176 succession of the Canadian High Arctic and the “10-million year flood,” in Piepjohn, K., Strauss, J.V.,
1177 Reinhardt, L., and McClelland, W.C., eds., Circum-Arctic Structural Events: Tectonic Evolution of the
1178 Arctic Margins and Trans-Arctic Links with Adjacent Orogens: Geological Society of America Special
1179 Paper 541, 1-18, doi:10.1130/2018.2541(11)

England, P., Houseman, G., 1986. Finite strain calculations of continental deformation: 2. Comparison with the India-Asia Collision Zone. Journal of Geophysical Research, Solid Earth, 91, 3664-3676. doi:10.1029/JB091iB03p03664

England, P., Houseman, G., Sonder, L., 1985. Length scales for continental deformation in convergent, divergent and strike-slip environments: Analytical and approximate solutions for a thin viscous sheet model. Journal of Geophysical Research, 90, 3551-3557.

England, P., McKenzie, D., 1982. A thin viscous sheet model for continental deformation. Geophysical Journal of the Royal Astronomical Society, 70, 295-321. doi:10.1111/j.1365-246X.1982.tb04969.x

Erlström, M., Thomas, S.A., Deeks, N., Sivhed, U., 1997. Structure and tectonic evolution of the Tornquist Zone and adjacent sedimentary basins in Scania and the southern Baltic Sea area. Tectonophysics, 271, 191-215.

Ervin, C.P., McGinnis, L.D., 1975. Reelfoot rift: reactivated precursor to the Mississippi Embayment. Geological Society of America Bulletin, 86, 1287-1295.

Fairhead, J.D., C.M. Green, S.M. Masterton, R. Guiraud, 2013. The role that plate tectonics, inferred stress changes and stratigraphic unconformities have on the evolution of the West and Central African Rift System and the Atlantic continental margins. Tectonophysics, 594, 118-127.

Faleide, J.I., Vågnes, E., Gudlaugsson, S.T., 1984. Late Mesozoic-Cenozoic evolution of the south-western Barents Sea in a regional rift-shear tectonic setting. Marine and Petroleum Geology, 10, 186-214.

Faleide, J.I., Gudlaugsson, S.T., Jacquart, G., 1993. Evolution of the western Barents Sea. Marine and Petroleum Geology, 1, 123-150.

Faure, S., Tremblay, A., Angelier, J., 1996. State of intraplate stress and tectonism of northeastern America since Cretaceous times, with particular emphasis on the New England-Quebec igneous province. Tectonophysics, 255, 111-134.

Fiedler, A., Faleide, J.I., 1996. Cenozoic sedimentation along the southwestern Barents Sea margin in relation to uplift and erosion of the shelf. Global and Planetary Change, 12, 75-93.

Finzel, E.S., Flesch, L.M., Ridgway, K.D., Holt, W.E., Ghosh, A., 2015. Surface motions and intraplate continental deformation in Alaska driven by mantle flow. Geophysical Research Letters, 42, 4350-4358. doi:10.1002/2015GL063987.

Flesch, L.M., Haines, A.J., Holt, W.E., 2001. Dynamics of the India-Eurasia collision zone. Journal of Geophysical Research, Solid Earth, 106, 16435-16460. doi:10.1029/2001JB000208

Fleitout, L., Froidevaux, C., 1983. Tectonic stresses in the lithosphere. Tectonics, 2, 315-324.

Foulger, G.R., Natland, J.H., Presnall, D.C., Anderson, D.L., Eds., 2005. Plates, Plumes, and Paradigms. Geological Society of America Special Volume 388, 881 pp.

Gabrielsen, R.H., Færseth, R.B., 1989. The inner shelf of North Cape, Norway and its implications for the Barents Shelf-Finnmark Caledonide boundary. A comment. Norsk Geologisk Tidskrift, 69, 57-62.

1216 Gabrielsen, R.H., Færseth, R.B., Jensen, L.N., Kalheim, J.E., Riis, F., 1990. Structural elements of the
1217 Norwegian continental shelf Part I, The Barents Sea Region, NPD-Bulletin, 6.

1218 Gabrielsen, R.H., Grunnaleite, I., Rasmussen, E., 1997. Cretaceous and Tertiary inversion in the
1219 Bjärnäyrenna Fault Complex, south-western Barents Sea. Marine and Petroleum Geology, 14, 165-
1220 178.

1221 Gaina, C., Jakob, J., 2019. Global Eocene tectonic unrest: possible causes and effects around the
1222 North American plate. Tectonophysics, 760, 136-151. doi:10.1016/j.tecto.2018.08.010

1223 Gaina, C., Nasuti, A., Kimbell, G.S., Blischke, A., 2017. Break-up and seafloor spreading domains in the
1224 NE Atlantic. Geological Society, London, Special Publications, 447, 393-417.

1225 Ghosh, A., Holt, W.E., Wen, L., 2013. Predicting the lithospheric stress field andplate motions by joint
1226 modeling of lithosphere and mantle dynamics. Journal of Geophysical Research, Solid Earth, 118,
1227 346-368. http://dx.doi.org/10.1029/2012JB009516

1228 Ghosh, A., Holt, W.E., Wen, L., Haines, A.J., Flesch, L.M., 2008. Joint modeling of lithosphere and
1229 mantle dynamics elucidating lithosphere-mantle coupling. Geophysical Research Letters, 35, L16309.
1230 doi:10.1029/2008GL034365

1231 Gołędowski, B., Nielsen, S.B., Clausen, O.R., 2012. Patterns of Cenozoic sediment flux from western
1232 Scandinavia. Basin Research, 24, 377-400. doi:10.1111/j.1365-2117.2011.00530.x

1233 Gregersen, U., Hopper, J.R., Knutz, P.C., 2013. Basin seismic stratigraphy and aspects of prospectivity
1234 in the NE Baffin Bay, Northwest Greenland. Marine and Petroleum Geology, 46, 1-8.

1235 Guiraud, M., 1993. Late Jurassic rifting – Early Cretaceous rifting and Late Cretaceous transpressional
1236 inversion in the upper Benue (NE Nigeria). Bull. Centres Rech. Explor.-Prod. Elf- Aquitaine, 17, 371-
1237 383.

1238 Guiraud, R., Binks, R.M., Fairhead, J.D., Wilson, M., 1992. Chronology and geodynamic setting of
1239 Cretaceous-Cenozoic rifting in West and Central Africa. Tectonophysics, 213, 227-234.

1240 Guiraud, R., Bosworth, W., 1997. Senonian basin inversion and rejuvenation of rifting in Africa and
1241 Arabia. Synthesis and implications to plate-scale tectonics. Tectonophysics, 282, 39-82.

1242 Guiraud, R., Bosworth, W., 1999. Phanerozoic geodynamic evolution of northeastern Africa and the
1243 northwestern Arabian platform. Tectonophysics, 315, 73-108

1244 Gutiérrez-Alonso, G., Fernández-Suárez, J., Weil, A.B., Murphy, J.B., Nance, R.D., Corfú, F., Johnston,
1245 S.T., 2008. Self-subduction of the Pangaean global plate. Nature Geoscience, 1, 549.

1246 Hamann, N.E., Whittaker, R.C, Stemmerik, L., 2005. Geological development of the Northeast
1247 Greenland Shelf. In: Doré, A.G., Vining, B. A. (eds). Petroleum Geology: North-West Europe and
1248 Global Perspectives—Proceedings of the 6th Petroleum Geology Conference, 887-902.

1249 Hand, M., Sandiford, M., 1999. Intraplate deformation in central Australia, the link between
1250 subsidence and fault reactivation. Tectonophysics, 305, 121-140.

1251 Handy, M.R., Schmid, S.M., Bousquet, R., Kissling, E., Bernoulli, D., 2010. Reconciling plate-tectonic
1252 reconstructions of Alpine Tethys with the geological-geophysical record of spreading and subduction
1253 in the Alps. Earth-Science Reviews, 102, 121-158.

1254 Hansen, D.L., Nielsen, S.B., 2003. Why rifts invert in compression. Tectonophysics, 373, 5-24.

1255 Harrison, J.C., T.A. Brent, G.N. Oakey, 2011. Baffin Fan and its inverted rift system of Arctic eastern
1256 Canada: stratigraphy, tectonics and petroleum resource potential. In: Spencer, A.M., Embry, A.F.,
1257 Gautier, D.L., Stoupakova, A.V., Sørensen, K. (eds) Arctic Petroleum Geology. Geological Society,
1258 London, Memoirs, 35, 595-626.

1259 Heidbach, O., Fuchs, K., Muller, B., Wenzel, F., Reinecker, J., Tingay, M., Sperner, B., 2007. The world
1260 stress map. Episodes, 30, 197-201.

1261 Heidbach, O., M. Rajabi, X. Cui, K. Fuchs, B. Müller, J. Reinecker, K. Reiter, M. Tingay, F. Wenzel, F.
1262 Xie, M.O. Ziegler, M.-L. Zoback and M.D. Zoback, 2018. The World Stress Map database release 2016:
1263 Crustal stress pattern across scales. Tectonophysics, 744, 484-498, doi:10.1016/j.tecto.2018.07.007

1264 Hengesh, J.V. and B.B. Whitney, 2016. Transcurrent reactivation of Australia's western passive
1265 margin: An example of intraplate deformation from the central Indo-Australian plate, Tectonics, 35,
1266 1066-1089. doi:10.1002/2015TC004103

1267 Henriksen, E., Ryseth, A.E., Larssen, G.B., Heide, T., Rønning, K., Sollid, K., Stoupakova, A.V. et al.,
1268 2011. Tectonostratigraphy of the greater Barents Sea: implications for petroleum systems, in: Embry,
1269 A.F., Gautier, D.L., Stoupakova, A.V., Sørensen, K. (eds) Arctic Petroleum Geology. Geological Society,
1270 London, Memoirs, 35, 163-195

1271 Heron, P.J., Peace, A.L., McCaffrey, K.J.W., Welford, J.K., Wilson, R.W., van Hunen, J., Pysklywec, R.N.,
1272 2019. Segmentation of rifts through structural inheritance: Creation of the Davis Strait. Tectonics, 38,
1273 2411-2430. doi:10.1029/2019TC005578.

1274 Heron, P.J., Pysklywec, R.N., Stephenson, R., 2015. Intraplate orogenesis within accreted and scarred
1275 lithosphere: example of the Eurekan Orogeny, Ellesmere Island. Tectonophysics, 664, 202-213,
1276 doi:10.1016/j.tecto.2015.09.011

1277 Heron, P.J., Pysklywec, R.N., Stephenson, R., 2016. Identifying mantle lithosphere inheritance in
1278 controlling intraplate orogenesis. Journal of Geophysical Research, Solid Earth, 121, 6966-6987,
1279 doi:10.1002/2016JB013460

1280 Hjelstuen, B.O., Elverhøi, A., Faleide, J.I., 1996. Cenozoic erosion and sediment yield in the drainage
1281 area of the Storfjorden Fan. Glob. Planet. Change, 12, 95-117.

1282 Höink, T., Jellinek, A.M., Lenardic, A., 2011. Viscous coupling at the lithosphere-asthenosphere
1283 boundary. Geochemistry, Geophysics, Geosystems, 12 (10). doi:10.1029/2011gc003698.

1284 Hosseinpour, M., Müller, R.D., Williams, S.E., Whittaker, J.M., 2013. Full-fit reconstruction of the
1285 Labrador Sea and Baffin Bay. Solid Earth, 4, 461-479. doi:10.5194/se-4-461-2013.

1286 Hurd, O., Zoback, M.D., 2012. Intraplate earthquakes, regional stress and fault mechanics in the
1287 Central and Eastern U.S. and southeastern Canada. Tectonophysics, 581, 182-192.
1288 doi:10.1016/j.tecto.2012.04.002.

1289 Izquierdo-Llavall, E., Menant, A., Aubourg, C., Callot, J.-P., Hoareau, G., Camps, P., Péré, E., Lahfid, A.,
1290 2020. Pre-orogenic folds and syn-orogenic basement tilts in an inverted hyperextended margin: the
1291 northern Pyrenees case study. Tectonics. doi:10.1029/2019TC005719

1292 Janssen, M.E., Stephenson, R.A., Cloetingh, S., 1995. Temporal and spatial correlations between
1293 changes in plate motions and the evolution of rifted basins in Africa. Geological Society of America
1294 Bulletin, 107, 1317-1332.

1295 Johnson, H., Ritchie, J.D., Hitchen, K., McInroy, D.B., Kimbell, G.S., 2005. January. Aspects of the
1296 Cenozoic deformational history of the Northeast Faroe-Shetland Basin, Wyville-Thomson Ridge and
1297 Hatton Bank areas. In Geological Society, London, Petroleum Geology Conference series, 6, 993-
1298 1007.

1299 Johnston, A.C., 1996. Seismic moment assessment of earthquakes in stable continental regions—III.
1300 New Madrid 1811-1812, Charleston 1886 and Lisbon 1755. Geophysical Journal International, 126,
1301 314-344. doi:10.1111/j.1365-246X.1996.tb05294.x.

1302 Jones, C.H., Unruh, J.R., Sonder, L.J., 1996. The role of gravitational potential energy in active
1303 deformation in the southwestern United States. Nature, 381, 37-41.

1304 Khriachtchevskaia, O., Stovba, S.M., Stephenson, R., 2010. Cretaceous-Cenozoic tectonic evolution of
1305 the Odessa Shelf and the Azov Sea from seismic data and 1-D modelling, in: M. Sosson, N. Kaymakci,
1306 R. Stephenson, V. Starostenko and F. Bergerat (Eds.), Sedimentary basin tectonics from the Black Sea
1307 and Caucasus to the Arabian Platform, Geological Society of London, Special Publication, 340, 137-
1308 147.

1309 Kimbell, G.S., M.A. Stewart, S. Gradmann, P.M. Shannon, T. Funck, C. Haase, M.S. Stoker, J.R. Hopper,
1310 2016. Controls on the location of compressional deformation on the NW European margin. In: Péron-
1311 Pinvidic, G., Hopper, J.R., Stoker, M.S., Gaina, C., Doornenbal, J.C., Funck, T., Árting, U.E. (eds), The NE
1312 Atlantic Region: A Reappraisal of Crustal Structure, Tectonostratigraphy and Magmatic Evolution.
1313 Geological Society, London, Special Publications, 447. doi:10.1144/SP447.3

1314 Kley, J., 2018. Timing and spatial patterns of Cretaceous and Cenozoic inversion in the Southern
1315 Permian Basin. In: Kilhams, B., Kukla, P.A., Mazur, S., Mckie, T., Mijnlieff, H.F., Van Ojik, K. (eds),
1316 Mesozoic Resource Potential in the Southern Permian Basin. Geological Society, London, Special
1317 Publications, 469, 19-31. doi:10.1144/SP469.12

1318 Kley, J., Voigt, T., 2008. Late Cretaceous intraplate thrusting in central Europe: effect of Africa-Iberia-
1319 Europe convergence, not Alpine collision. Geology, 36, 839-842.

1320 Kockel, F, 2003. Inversion structures in Central Europe – expressions and reasons, an open discussion.
1321 Netherlands Journal of Geosciences, 82, 367-382.

Koehl, J.B., Bergh, S.G., Henningsen, T., Faleide, J-I., 2018. Middle to Late Devonian-Carboniferous collapse basins on the Finnmark Platform and in the southwesternmost Nordkapp basin, SW Barents Sea, Solid Earth, 9, 341-372

Krzywiec, P., Stachowska, A., 2016. Late Cretaceous inversion of the NW segment of the Mid-Polish Trough – how marginal troughs were formed, and does it matter at all? Z. Dt. Ges. Geowiss., 167, 107-119.

Le Breton, E., Cobbold, P.R., Dauteuil, O., and Lewis, G., 2012. Variations in amount and direction of seafloor spreading along the northeast Atlantic Ocean and resulting deformation of the continental margin of northwest Europe. Tectonics, 31, 1-16, doi:10.1029/2011TC003087

Levandowski, W., Boyd, O.S., Ramirez-Guzmán, L., 2016. Dense lower crust elevates long-term earthquake rates in the New Madrid seismic zone. Geophysical Research Letters, 43, 8499-8510. doi:10.1002/2016GL070175.

Levandowski, W., Herrmann, R.B., Briggs, R., Boyd, O., Gold, R., 2018. An updated stress map of the continental United States reveals heterogeneous intraplate stress. Nature Geoscience, 11, 433-437.

Lithgow-Bertelloni, C., Guynn, J.H., 2004. Origin of the lithospheric stress field. Journal of Geophysical Research: Solid Earth, 109(B1).

Liu, L., Zoback, M.D., 1997. Lithospheric strength and intraplate in the New Madrid seismic zone seismicity. Tectonics, 16, 585-595.

Lu, G., Zhao, L., Zheng, T., Kaus, B.J.P., 2013. Strong intracontinental lithospheric deformation in South China: Implications from seismic observations and geodynamic modelling. Journal of Asian Earth Sciences, 86, 106-116.

Lundin, E.R., Doré, A.G., 2002. Mid-Cenozoic post-break-up deformation in the 'passive' margins bordering the Norwegian-Greenland Sea. Marine and Petroleum Geology, 19, 79-93.

Lundin, E.R., Doré, A.G., 2005. NE Atlantic break-up: a re-examination of the Iceland mantle plume model and the Atlantic–Arctic linkage. In: Doré, A.G., Vining, B.A. (eds) Petroleum Geology: North-West Europe and Global Perspectives—Proceedings of the 6th Petroleum Geology Conference, 739-754. Geological Society, London.

Marotta, A.M., Sabadini, R., 2003. Numerical models of tectonic deformation at the Baltica-Avalonia transition zone during the Palaeocene phase of inversion. Tectonophysics, 373, 25-37

Marshak, S., Karlstrom, K., Timmons, J.M., 2000. Inversion of Proterozoic extensional faults: An explanation for the pattern of Laramide and Ancestral Rockies intracratonic deformation, United States. Geology, 28, 735738.

Maystrenko, Yuriy, Sergiy Stovba, Randell Stephenson, Ulf Bayer, Elive Menyoli, Dirk Gajewski, Christian Huebscher, Wolfgang Rabbel, Aline Saintot, Vitaliy Starostenko, Hans Thybo, Anatoliy Tolkunov, 2003. Crustal-scale pop-up structure in cratonic lithosphere: DOBRE deep seismic reflection study of the Donbas Foldbelt, Ukraine. Geology, 31, 733-736.

Mazzotti, S., Gueydan, F., 2018. Control of tectonic inheritance on continental intraplate strain rate and seismicity. Tectonophysics, 746, 602-610.

McIntyre, D., Ricketts, B.D., 1989. New palynological data concerning Cornwall Arch from Cornwall and Amund Ringnes Islands, District of Franklin. Geol. Surv. Can. Pap., 89-1G: 199 202.

Miller, K.G., Kominz, M.A., Browning, J.V., Wright, J.D., Mountain, G.S., Katz, M.E., Sugarman, P.J., Cramer, B.S., Christie-Blick, N., Pekar, S.F., 2005. The Phanerozoic record of global sea-level change. Science 310, 1293-1298.

Mooney, W.D., Andrews, M.C., Ginzburg, A., Peters, D.A., Hamilton, R.M., 1983. Crustal structure of the northern Mississippi Embayment and a comparison with other continental rift zones. Tectonophysics, 94, 327-348.

Mogensen, T.E., 1994. Palaeozoic structural development along the Tornquist Zone, Kattegat area, Denmark. Tectonophysics, 240, 191-214.

Mogensen, T.E., Korstgård, J.A., 2003. Triassic and Jurassic transtension along part of the Sorgenfrei-Tornquist Zone in the Danish Kattegat, Geological Survey of Denmark and Greenland Bulletin, 1, 439-458.

Molnar, P., England, P.C., and Jones, C.H., 2015. Mantle dynamics, isostasy, and the support of high terrain. Journal of Geophysical Research, Solid Earth, 120, 19321957. doi:10.1002/2014JB011724

Mosar, J., Lewis, G. Torsvik, T., 2002. North Atlantic seafloor spreading rates: implications for the Tertiary development of inversion structures of the Norwegian-Greenland Sea. Journal of the Geological Society, 159, 503-515. doi:10.1144/0016-764901-135

Moustafa, A.R., 2013. Fold-related faults in the Syrian Arc belt of northern Egypt. Marine and Petroleum Geology, 48, 441-454.

Muir-Wood, R., 2000. Deglaciation Seismotectonics: a principal influence on intraplate seismogenesis at high latitudes. Quaternary Science Reviews, 19, 1399-1411.

Müller, R.D., Sdrolias, M., Gaina, C., Roest, W.R., 2008. Age, spreading rates, and spreading asymmetry of the world's ocean crust. Geochem. Geophys. Geosystems 9, Q04006. doi:10.1029/2007GC001743

Murphy, B.S., Liu, L., Egbert, G.D., 2019. Insights into intraplate stresses and geomorphology in the southeastern United States. Geophysical Research Letters, 46, 8711-8720. doi:10.1029/2019GL083755

Nielsen, S.B., Hansen, D.L., 2000. Physical explanation of the formation and evolution of inversion zones and marginal troughs. Geology, 28, 875-878.

Nielsen, S.B., Stephenson, R.A., Thomsen, E., 2007. Dynamics of Mid-Palaeocene North Atlantic rifting linked with European intra-plate deformations. Nature, 450, 1071-1074.

Nielsen, S.B., Stephenson, R., Schiffer, C., 2014. Deep controls on intraplate basin inversion, in: Talwani, P. (Ed.), Intraplate Earthquakes. Cambridge University Press.

1394 Nielsen, S.B., Thomsen, E., Hansen, D.L., Clausen, O.R., 2005. Plate-wide stress relaxation explains
1395 European Palaeocene basin inversions. Nature, 435, 195-198.

1396 Nøttvedt, A., Livbjerg, F., Midbøe, S., 1988. Tertiary deformation of Svalbard – various models and
1397 recent advances in: W.K. Dallmann, Y. Ohto, A. Andresen (editors), Tertiary Tectonics of Svalbard,
1398 Norsk Polarinstitutt, Rapportserie, 46.

1399 Oakey, G.N., Chalmers, J.A., 2012. A new model for the Paleogene motion of Greenland relative to
1400 North America: Plate reconstructions of the Davis Strait and Nares Strait regions between Canada
1401 and Greenland, Journal of Geophysical Research, 117, B10401. doi:10.1029/2011JB008942

1402 Peace, A.L., Dempsey, E.D., Schiffer, C., Welford, J.K., McCaffrey, K., Imber, J., Phethean, J., 2018a.
1403 Evidence for basement reactivation during the opening of the Labrador Sea from the Makkovik
1404 Province, Labrador, Canada: insights from field data and numerical models. Geosciences, 8, 308.

1405 Peace, A., McCaffrey, K., Imber, J., Hunen, J. Van, Hobbs, R., Wilson, R., 2018b. The role of pre-
1406 existing structures during rifting, continental break-up and transform system development, offshore
1407 West Greenland, Basin Research, 30, 373-394. doi:10.1111/bre.12257

1408 Pedrera, A., García-Senz, J., Ayala, C., Ruiz-Constán, A., Rodríguez-Fernández, L.R., Robador, A.,
1409 González Menéndez, L., 2017. Reconstruction of the Exhumed Mantle Across the North Iberian
1410 Margin by Crustal-Scale 3-D Gravity Inversion and Geological Cross Section: Tectonics, 12,
1411 2017TC004716. doi:10.1002/2017TC004716

1412 Petersen, K.D., Nielsen, S.B., Clausen, O.R., Stephenson, R., Gerya, T., 2010. Small-scale mantle
1413 convection produces stratigraphic sequences in sedimentary basins. Science, 329, 827-830.

1414 Phethean, J.J.J., L.M Kalnins, J. van Hunen, P.G. Biffi, R.J. Davies, K.J.W. McCaffrey, 2016.
1415 Madagascar's escape from Africa: A high-resolution plate reconstruction for the Western Somali
1416 Basin and implications for supercontinent dispersal, Geochem. Geophys. Geosyst., 17, 5036-5055.
1417 doi:10.1002/2016GC006624.

1418 Piepjohn, K., von Gosen, W., Tessensohn, F., 2016. The Eurekan deformation in the Arctic: an outline.
1419 Journal of the Geological Society, 173, 1007-1024, doi:10.1144/jgs2016-081

1420 Piepjohn, K., von Gosen, W., Tessensohn, F., Reinhardt, L., McClelland, W.C., Dallmann, W., Gädicke,
1421 C., Harrison, J.C., 2015. Tectonic map of the Ellesmerian and Eurekan deformation belts on Svalbard,
1422 north Greenland, and the Queen Elizabeth Islands (Canadian Arctic). Arktos, 1, 12.

1423 Pinet, N., 2016. Far-field effects of Appalachian orogenesis: a view from the craton. Geology, 44, 83-
1424 86.

1425 Raimondo, T., Hand, M., Collins, W.J., 2014. Compressional intracontinental orogens: Ancient and
1426 modern perspectives. Earth-Science Reviews, 130, 128-153.

1427 Rajabi, M., Tingaya, M., Heidbach, O., Hillis, R., Reynolds, S., 2017. The present-day stress field of
1428 Australia. Earth-Science Reviews, 168, 165-189.

1429 Ranalli, G., 1995. Rheology of the Earth. Chapman and Hall in London, New York.

Ritchie, J.D., Johnson, H., Quinn, M.F., Gatliff, R.W., 2008. The effects of Cenozoic compression within the Faroe-Shetland Basin and adjacent areas. Geological Society, London, Special Publications, 306, 121-136.

Roberts, D.G., Bally, A.W. eds., 2012. Regional geology and tectonics: Phanerozoic passive margins, cratonic basins and global tectonic maps (Vol. 1). Elsevier.

Rodríguez-Salgado, P., Childs, C., Shannon, P.M., Walsh, J.J., 2017. Structural controls on different styles of Cenozoic inversion in the Celtic Sea basins, offshore Ireland: 79th EAGE Conference and Exhibition 2017, June 2017, 12-15, doi:10.3997/2214-4609.201701288.

Rosenbaum, G., Lister, G.S., Duboz, C., 2002. Relative motions of Africa, Iberia and Europe during Alpine orogeny. Tectonophysics, 359, 117-129.

Rybacki, E., Evans, B., Janssen, C., Wirth, R., Dresen, G., 2013. Influence of stress, temperature, and strain on calcite twins constrained by deformation experiments. Tectonophysics, 601, 20-36.

Ryseth, A., Augustson, J.H., Charnock, M., Haugerud,O., Knutsen, S.-M., Midbøe, P.S., Opsal, J.G., Sundsbø, G., 2003. Cenozoic stratigraphy and evolution of the Sørvestsnaget Basin, southwestern Barents Sea. Norwegian Journal of Geology, 83, 107-130.

Saintot, A., M-F. Brunet, F. Yakovlev, M. Sébrier, R.A. Stephenson, A. Ershov, F. Chalot-Prat, T. McCann, 2006. The Mesozoic-Cenozoic tectonic evolution of the Greater Caucasus, in: D.G. Gee and R.A. Stephenson (Eds.), European Lithosphere Dynamics, Geological Society of London, Memoir 32, 277-289.

Saintot, A., Stephenson, R., Brem, A., Stovba, S., Privalov, V., 2003. Paleostress field reconstruction and revised tectonic history of the Donbas fold-and-thrust belt (Ukraine and Russia). Tectonics, 22 (5). doi:10.1029/2002TC001366

Saintot, A., Stephenson, R., Stovba, S., Maystrenko, Y., 2003. Structures associated with inversion of the Donbas Foldbelt (Ukraine and Russia). Tectonophysics, 373, 181-207.

Sandiford, M., 1999. Mechanics of basin inversion. Tectonophysics, 305, 109-120.

Sandiford, M., Hansen, D.L., McLaren, S.N., 2006. Lower crustal rheological expression in inverted basins, in Buiter, S.J.H., Schreurs, G. (eds). Analogue and Numerical Modelling of Crustal-Scale Processes. Geological Society, London, Special Publications, 253, 271-283.

Sandiford, M., Quigley, M., 2009. TOPO-OZ: Insights into the various modes of intraplate deformation in the Australian continent. Tectonophysics, 474, 405-416. doi:10.1016/j.tecto.2009.01.028

Sættem, J., Bugge, T., Fanavoll, S., Goll, R.M., Mork, A., Mork, M.B.E., Smelror, M., Verdenius, J.G., 1994. Cenozoic margin development and erosion of the Barents Sea: core evidence from southwest of Bjornoya, Marine Geology, 118, 257-281

Schack-Pedersen, S.A., Häkansson, E., 2001. Kronprins Christian land orogeny deformational styles of the end Cretaceous transpressional mobile belt in eastern North Greenland. Polarforschung, 69, 117-130.

Scheck-Wenderoth, M., Krzywiec, P., Zülke, R., Maystrenko, Y., Frizheim, N., 2008. Permian to Cretaceous tectonics. In: McCann, T. (ed.): The Geology of Central Europe; vol. 2: Mesozoic and Cenozoic, 999-1030, Geological Society, London.

Scheck-Wenderoth, M., Lamarche, J., 2005. Crustal memory and basin evolution in the Central European Basin System—new insights from a 3D structural model. Tectonophysics, 397, 143-165. doi:10.1016/j.tecto.2004.10.007

Schiffer, Christian, Anthony G. Doré, Gillian R. Foulger, Dieter Franke, Laurent Geoffroy, Laurent Gernigon, Bob Holdsworth, Nick Kusznir, Erik Lundin, Ken McCaffrey, Alex Peace, Kenni D. Petersen, Thomas Phillips, Randell Stephenson, Martyn S. Stoker, Kim Welford, 2019a. Structural inheritance in the North Atlantic. Earth-Science Reviews. doi:10.1016/j.earscirev.2019.102975

Schiffer, C., Nielsen, S.B., 2016. Implications for anomalous mantle pressure and dynamic topography from lithospheric stress patterns in the North Atlantic Realm. Journal of Geodynamics, 98, 53-69. doi:10.1016/j.jog.2016.03.014

Schiffer, Christian, Alexander Peace, Jordan Phethean, Laurent Gernigon, Ken McCaffrey, Kenni D. Petersen, Gillian Foulger, 2019b. The Jan Mayen microplate complex and the Wilson cycle. In: Wilson, R.W., Houseman, G.A., McCaffrey, K.J.W., Doré, A.G., Buiter, S.J.H. (eds). Fifty Years of the Wilson Cycle Concept in Plate Tectonics. Geological Society, London, Special Publications, 470, 393-414. doi:10.1144/SP470.2

Schiffer, C., Tegner, C., Schaeffer, A.J., Pease, V., Nielsen, S.B., 2018. High Arctic geopotential stress field and implications for geodynamic evolution. Geological Society, London, Special Publications, 460, 441-465.

Scotese, C.R., 2016. PALAEOMAP PalaeoAtlas for GPlates and the PalaeoData Plotter Program. PALAEOMAP Project. http://www.earthbyte.org/palaeomap-palaeoatlas-forgplates/

Sella, G.F., Stein, S., Dixon, T.H., Craymer, M., James, T.S., Mazzotti, S., Dokka, R.K., 2007. Observation of glacial isostatic adjustment in “stable” North America with GPS. Geophysical Research Letters, 34, 1-6.

Seton, M., Müller, R.D., Zahirovic, S., Gaina, C., Torsvik, T., Shephard, G., Talsma, A., Gurnis, M., Turner, M., Maus, S., Chandler, M., 2012. Global continental and ocean basin reconstructions since 200 Ma. Earth-Science Reviews, 113, 212-270. doi:10.1016/j.earscirev.2012.03.002

Shaw, R.D., Etheridge, M.A., Lambeck, K., 1991. Development of the late Proterozoic to mid-Palaeozoic intracratonic Amadeus Basin in central Australia: a key to understanding tectonic forces in plate interiors. Tectonics, 10, 688-721.

Sheremet, Ye., Marc Sosson, Gueorgui Ratzov, Grigoriy Sydorenko, Zinoviy Voitsitskiy, Tamara Yegorova, Oleg Gintov, Anna Murovskaya, 2016. An offshore-onland transect across the north-eastern Black Sea basin (Crimean margin): Evidence of Palaeocene to Pliocene two-stage compression. Tectonophysics, 688, 84-100. doi:10.1016/j.tecto.2016.09.015

Skaarup, N., Pulvertaft, C.R., 2007. Aspects of the structure on the coast of the West Greenland volcanic province revealed in seismic data. Bulletin of the Geological Society of Denmark, 55.

Smallwood, J.R., 2004. Tertiary inversion in the Faroe-Shetland Channel and the development of major erosional scarps. Geological Society, London, Memoirs, 29, 187-198.

Smallwood, J.R., Kirk, W.J., 2005. Palaeocene exploration in the Faroe-Shetland Channel: disappointments and discoveries. Geological Society, London, Petroleum Geology Conference series, 6, 977-991.

Sørensen, E.V., Hopper, J.R., Pedersen, G.K., Nøhr-Hansen, H., Guarnieri, P., Pedersen, A.K., Christiansen, F.G., 2017. Inversion structures as potential petroleum exploration targets on Nuussuaq and northern Disko, onshore West Greenland. Geological Survey of Denmark and Greenland Bulletin, 38, 45-48.

Sosson, Marc, Randell Stephenson, Yevgeniya Sheremet, Yann Rolland, Shota Adamia, Rafael Melkonian, Talat Kangarli, Tamara Yegorova, Ara Avagyan, Ghazar Galoyan, Taniel Danelian, Marc Hässig, Maud Meijers, Carla Müller, Lilit Sahakyan, Nino Sadradze, Victor Alania, Onice Enukidze, Jon Mosar, 2016. The eastern Black Sea-Caucasus region during the Cretaceous: New evidence to constrain its tectonic evolution. C. R. Geoscience, 348, 23-32, doi:10.1016/j.crte.2015.11.002

Starostenko, V., T. Janik, R. Stephenson, D. Gryn, O. Rusakov, W. Czuba, P. Środa, M. Grad, A. Guterch, E. Flüh, H. Thybo, I. Artemieva, A. Tolkunov, G. Sydorenko, D. Lysynchuk, V. Omelchenko, K. Kolomiyets, O. Legostaeva, A. Dannowski, A. Shulgin, 2016. DOBRE-2 WARR profile: the Earth's crust across Crimea between the pre-Azov Massif and the northeastern Black Sea Basin. In: Sosson, M., Stephenson, R.A., Adamia, S.A. (eds), Tectonic Evolution of the Eastern Black Sea and Caucasus. Geological Society of London, Special Publication, 428, 199-220, doi:10.1144/SP428.11

Stephenson, R.A., A. Chekunov, T. Ilchenko, L. Kaluzhna, Ye. Baranova, V. Starostenko, S. Krasovskiy, V. Kozlenko, P. Kuprienko, V. Gordienko, R. Kutas, I. Pashkevich, M. Orluk, M.K. Kivshik, S.M. Stovba, M.T. Turchanenko, V.I. Savchenko, B.S. Krivchenkov, M. Narkiewicz, R. Dadlez, J. Pokorski, A. Guterch, 1993. Continental Rift Development in Precambrian and Phanerozoic Europe: EUROPROBE and the Dnieper-Donets Rift and Polish Trough basins. Sedimentary Geology, 86, 159-175.

Stephenson, R., Egholm, D.L., Nielsen, S.B., Stovba, S.M., 2009. Thermal refraction facilitates 'cold' intra-plate deformation: The Donbas foldbelt (Ukraine). Nature Geosciences, 2, 290-293.

Stephenson, R., Lambeck, K., 1985. Isostatic response of the lithosphere with in-plane stress: application to central Australia. Journal of Geophysical Research, 90, 8581-8588.

Stephenson, R., K. Piepjohn, C. Schiffer, W. von Gosen, G.N. Oakey, G. Anudu, 2017. Integrated crustal-geological cross-section of Ellesmere Island. In: Pease, V., Coakley, B. (eds). Circum-Arctic Lithosphere Evolution. Geological Society, London, Special Publications, 460, 7-17. doi.org/10.1144/SP460.12

Stephenson, R., Schellart, W.P., 2010. The Black Sea back-arc basin: insights to its origin from geodynamic models of modern analogues. in: M. Sosson, N. Kaymakci, R. Stephenson, V. Starostenko and F. Bergerat (Eds.), Sedimentary basin tectonics from the Black Sea and Caucasus to the Arabian Platform, Geological Society, London, Special Publications, 340, 11-21.

Stoker, M.S., Doornenbal, H., Hopper, J.R., Gaina, C., 2014. Tectonostratigraphy. In: Hopper, J.R., Funck, T., Stoker, M.S., Árting, U., Peron-Pinvidic, G., Doornenbal, H., Gaina, C. (eds) Tectonostratigraphic Atlas of the North-East Atlantic Region. Geological Survey of Denmark and Greenland, GEUS, Copenhagen, 129-212.

Stoker, M.S., Simon P. Holford, Richard R. Hillis, 2017. A rift-to-drift record of vertical crustal motions in the Faroe-Shetland Basin, NW European margin: establishing constraints on NE Atlantic evolution. J. Geol. Soc. Lon. doi:10.1144/jgs2017-076

Stovba, S.M., Popadyuk, I.V., Khriachtchevskaia, O.I., Fenota, P.O., 2017a. The Ukrainian Sector of the Black Sea and Crimea: The Atlas of Subcrop Maps and Palaeogeographical Reconstructions. Abstracts of EAGE conference Geoinformatics, Kyiv, 20-24. Doi:10.3997/2214-4609.201701799

Stovba, S.M., Popadyuk, I.V., Khriachtchevskaia, O.I., Fenota, P.O., 2017b. Crimea and Ukrainian Black Sea: the origin, tectonics and evolution. Abstracts of EAGE conference Geoinformatics, Kyiv, p. 577-581. doi:10.3997/2214-4609.201701798

Stovba, S.M., Stephenson, R.A., 1999. The Donbas Foldbelt: its relationships with the uninverted Donets segment of the Dniepr-Donets Basin, Ukraine. Tectonophysics, 313, 59-83.

Sund, T., O. Skarpnes, L.N, Jensen, R.M. Larsen, 1986, Tectonic Development and Hydrocarbon Potential Offshore Troms, Northern Norway, AAPG Special Volumes, Memoirs, A131, 615-627

Sutherland, R., J. Collot, F. Bache, S. Henrys, D. Barker, G.H. Browne, M.J.F. Lawrence, H.E.G. Morgans, C.J. Hollis, C. Clowes, N. Mortimer, P. Rouillard, M. Gurnis, S. Etienne, W. Stratford, 2017. Widespread compression associated with Eocene Tonga-Kermadec subduction initiation. Geology, 45, 355-358. doi:10.1130/G38617.1

Svennevig, K., Guarnieri, P., Stemmerik, L., 2016. Tectonic inversion in the Wandel Sea Basin: A new structural model of Kilen (eastern North Greenland). Tectonics, 35, 2896-2917.

Talwani, P. (Ed.), 2014. *Intraplate Earthquakes*. Cambridge: Cambridge University Press. doi:10.1017/CBO9781139628921

Tarantola, A., Valette, B., 1982. Generalized nonlinear inverse problems solved using the least squares criterion. Rev. Geophys. 20, 219-232. doi:10.1029/RG020i002p00219

Thiede, J., Diesen, G.W., Knudsen, B.-E., Snöre, T., 1986. Patterns of Cenozoic sedimentation in the Norwegian-Greenland Sea. Marine Geology, 69, 323-352.

Turner, J.P., Williams, G.A, 2004. Sedimentary basin inversion and intraplate shortening, Earth-Science Reviews, 65, 277-304.

Tuttle, Martitia P., Schweig, Eugene S., John D. Sims, Lafferty, Robert H., Wolf, Lorraine W., Hayes, Marion L., 2002. The Earthquake Potential of the New Madrid Seismic Zone. Bulletin of the Seismological Society of America, 92, 2080-2089.

Underhill, J.R., Paterson, S., 1998. Genesis of tectonic inversion structures: seismic evidence for the development of key structures along the Purbeck-Isle of Wight Disturbance: Journal of the Geological Society, 155, 975-992.

Ur-Rehman, 2012. Structural Analysis of the Knølegga Fault Complex, NW Barents Sea., Master's Thesis, Department of Geosciences, University of Oslo.

Vågnes, E., Gabrielsen, R.H., Haremo, P., 1998. Late Cretaceous-Cenozoic intraplate contractional deformation at the Norwegian continental shelf: timing, magnitude and regional implications. Tectonophysics, 300, 29-46.

van Buchem F.S.P., Smit, F.W.H., Buijs, G.J.A., Trudgill, B., Larsen, P.H., 2018. Tectonostratigraphic framework and depositional history of the Cretaceous-Danian succession of the Danish Central Graben (North Sea) – new light on a mature area. Geological Society, London, Petroleum Geology Conference series, 8, 9-46

van der Pluijm, B.A., Craddock, J.P., Graham, B.R., Harris, J.H., 1997. Paleostress in cratonic North America: implications for deformation of continental interiors. Science, 277, 794-796.

van Hoorn, B. 1987. Structural evolution, timing and tectonic style of the Sole Pit inversion. Tectonophysics, 137, 239-284.

Vejbæk, O.V., Andersen, C., 1987. Cretaceous-Early Tertiary inversion tectonism in the Danish Central Trough, Tectonophysics, 137, 221-238

Vejbæk. O.V., Andersen, C., 2002. Post mid-Cretaceous inversion tectonics in the Danish Central Graben – regionally synchronous tectonic events? Bulletin of the Geological Society of Denmark, 49, 93-204.

Voigt, E., 1962. Über Randtröge vor Schollenrändern und ihre Bedeutung im Gebiet der Mitteleuropäischen Senke und angrenzender Gebiete. Z. Deutsch. Geol. Gesell., 114, 378-418.

Welford, J.K., Peace, A.L., Geng, M., Dehler, S.A. Dickie, K., 2018. Crustal structure of Baffin Bay from constrained three-dimensional gravity inversion and deformable plate tectonic models. Geophysical Journal International, 214 (2). doi: 10.1093/gji/ggy193

Whittaker, R.C., Hamann, N.E., Pulvertaft, T.C.R., 1997. A new frontier province offshore northwest Greenland: Structure, basin development, and petroleum potential of the Melville Bay area: AAPG Bulletin, 81, 978-998, doi:10.1306/522B49B5-1727-11D7-8645000102C1865D.

Williams, G.A., Turner, J.P., Holford, S.P., 2005. Inversion and exhumation of the St. George's Channel basin, offshore Wales, UK. Journal of the Geological Society, 162, 97-110.

Wilson, R.W., Klint, K.E.S., Van Gool, J.M., McCaffrey, K.J.W., Holdsworth, R.E., Chalmers, J.A., 2006. Faults and fractures in central West Greenland: onshore expression of continental break-up and seafloor spreading in the Labrador-Baffin Bay Sea: Geological Survey of Denmark and Greenland Bulletin, 11, 185-204.

Wold, C.N., 1994. Cenozoic sediment accumulation on drifts in the northern North Atlantic. Paleoceanography, 9, 917-941.

Wolf, T.C.W., Thiede, J., 1991. History of terrigenous sedimentation during the past 10 m.y. in the North Atlantic (ODP Legs 104 and 105 and DSDP Leg 81). Mar. Geol., Cenozoic Geology of the

1614 Northwest European Continental Margin and Adjacent Deep-Sea Areas 101, 83-102.
1615 doi:10.1016/0025-3227(91)90064-B

1616 Ziegler, P.A., 1987. Late Cretaceous and Cenozoic intra-plate compressional deformations in the
1617 Alpine foreland - a geodynamic model. Tectonophysics, 137, 389-420.

1618 Ziegler, P.A., 1988. Evolution of the Arctic-North Atlantic and western Tethys, Am. Assoc. Petrol.
1619 Geol. Mem., 43, 198 p.

1620 Ziegler, P.A., 1990. Geological Atlas of Western and Central Europe, 2nd Ed. Shell Internationale
1621 Petroleum Mij. B.V. and Geological Society of London Publishing House, Bath, England, 239 p.

1622 Ziegler, P.A, Bertotti, G., Cloetingh, S., 2002. Dynamic processes controlling foreland development -
1623 the role of mechanical (de)coupling of orogenic wedges and forelands. EGU Stephan Mueller Special
1624 Publication Series, 1, 17-56.

1625 Ziegler, P.A., Cloetingh, S., van Wees, J-D., 1995. Dynamics of intraplate compressional deformation:
1626 The Alpine foreland and other examples. Tectonophysics, 252, 7-59.

1627 Ziegler, P.A., Schumacher, M.E., Dèzes, P., van Wees, J-D., Cloetingh, S., 2006. Post-Variscan
1628 evolution of the lithosphere in the area of the European Cenozoic Rift System. In European
1629 Lithosphere Dynamics ed. D.G. Gee and R.A. Stephenson. Geological Society, London, Memoirs, 32,
1630 97-112.

1631 Zienkiewicz, 1977. The Finite Element Method, 3rd ed. McGraw-Hill, Maidenhead, Berkshire,
1632 England.

1633 Ziska, H., Varming, T., 2008. Palaeogene evolution of the Ymir and Wyville Thomson ridges, European
1634 North Atlantic margin. Geological Society, London, Special Publications, 306, 153-168.

1635

1636

Figures

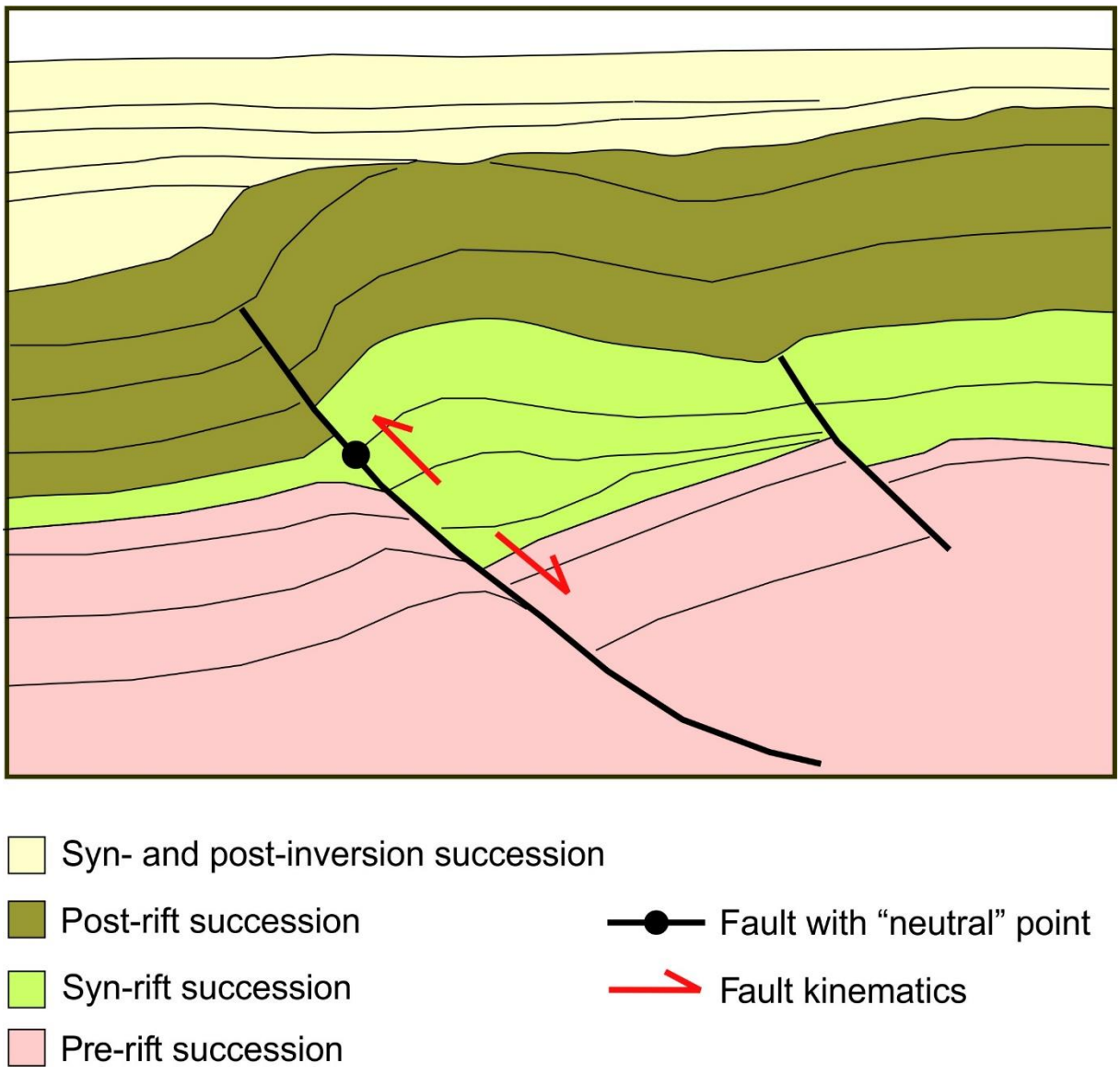

Figure 1. Basin inversion, based on a seismically imaged inverted half-graben in the East Java Sea basin, Indonesia (from Turner and Williams, 2004). An originally normal fault (lower kinematic indicator), forming a half-graben during tectonic extension, has later been reactivated as a reverse fault (upper kinematic indicator). There is no net offset of strata at the “neutral” point. See text for more explanation.

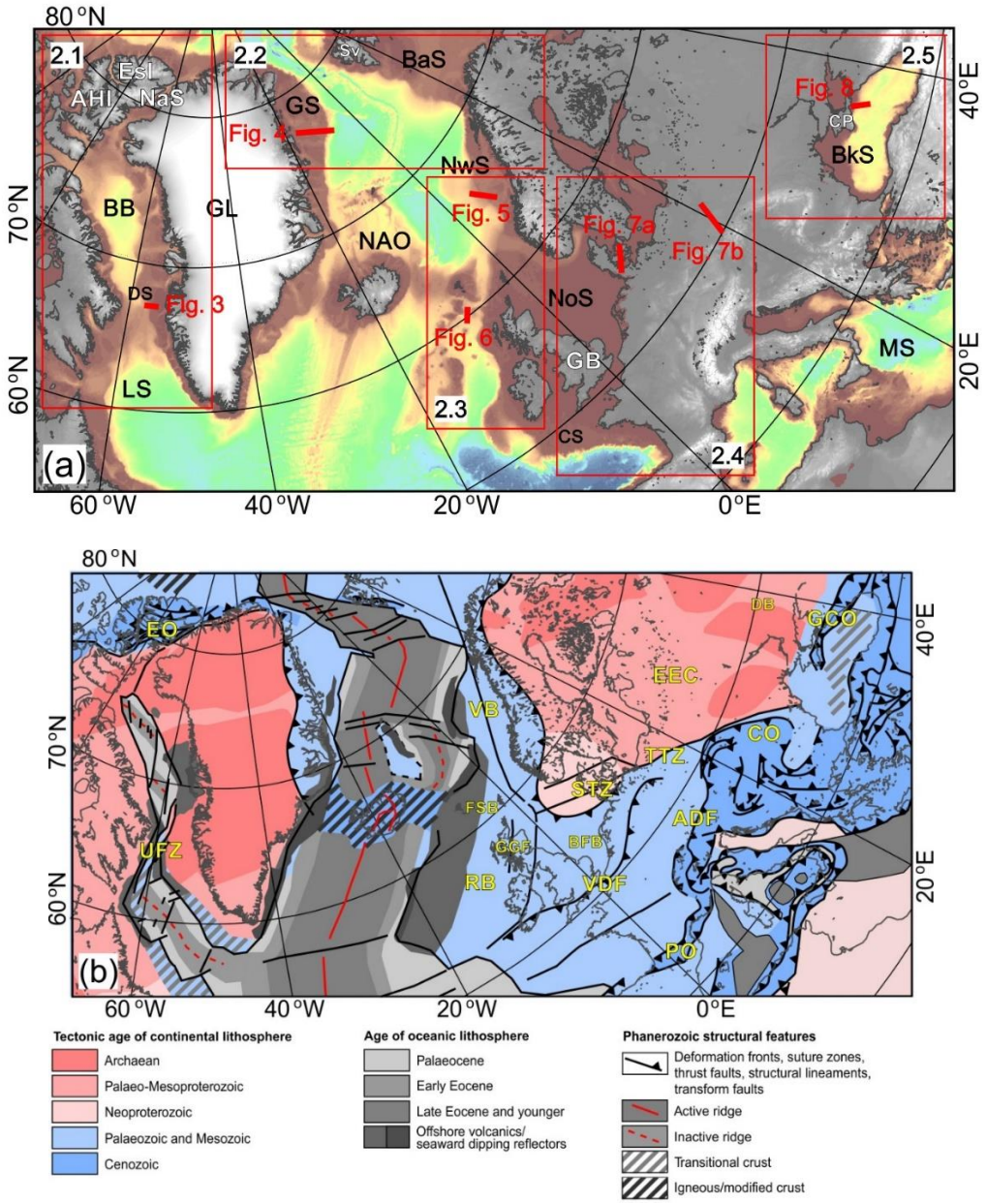

Figure 2. (a) The North Atlantic-western Alpine-Tethys study realm, showing regions in which the record of intraplate deformation is discussed in sub-sections 2.1-2.5 (red boxes, as labelled) and the locations of example basin inversion structures of various ages imaged on interpreted seismic reflection profiles in Figure 3-8, as labelled. Also seen are geographic elements mentioned in the text: AHI – Axel Heiberg Island; BaS – Barents Sea; BkS – Black Sea; BB – Baffin Bay; CP – Crimean Peninsula; CS – Celtic Sea; DS – Davis Strait; Esl – Ellesmere Island; GB – Great Britain; GL – Greenland; GS – Greenland Sea; LS – Labrador Sea; MS – Mediterranean Sea; NOA – North Atlantic Ocean; NaS – Nares Strait; NoS- North Sea; NwS – Norwegian Sea; Sv – Svalbard. (b) Tectonic overview of the study realm (oceanic lithosphere age of formation; continental lithosphere age of youngest tectonic overprint, compiled from Chauvet et al., 2019; Gaina et al., 2017; Handy et al., 2020; Piepjohn et al., 2015; Roberts and Bally, 2012; Schiffer et al., 2019a,b; Stephenson and Schellart, 2010) and the locations of tectonic elements mentioned in the text: ADF – Alpine Deformation Front; BFB – Broad Fourteens Basin; DB – Donbas Basin; CO – Carpathian Orogen; EEC – East European Craton; EO – Eurekan Orogen; FSB – Faroe-Shetland basin; GCO – Greater Caucasus Orogen; GGF – Great Glen Fault; STZ – Sorgenfrei- Tornquist Zone; TTZ – Tornquist-Tesseyre Zone, UFZ – Ungava Fault Zone; VB – Vøring Basin; VDF – Variscan Deformation Front.

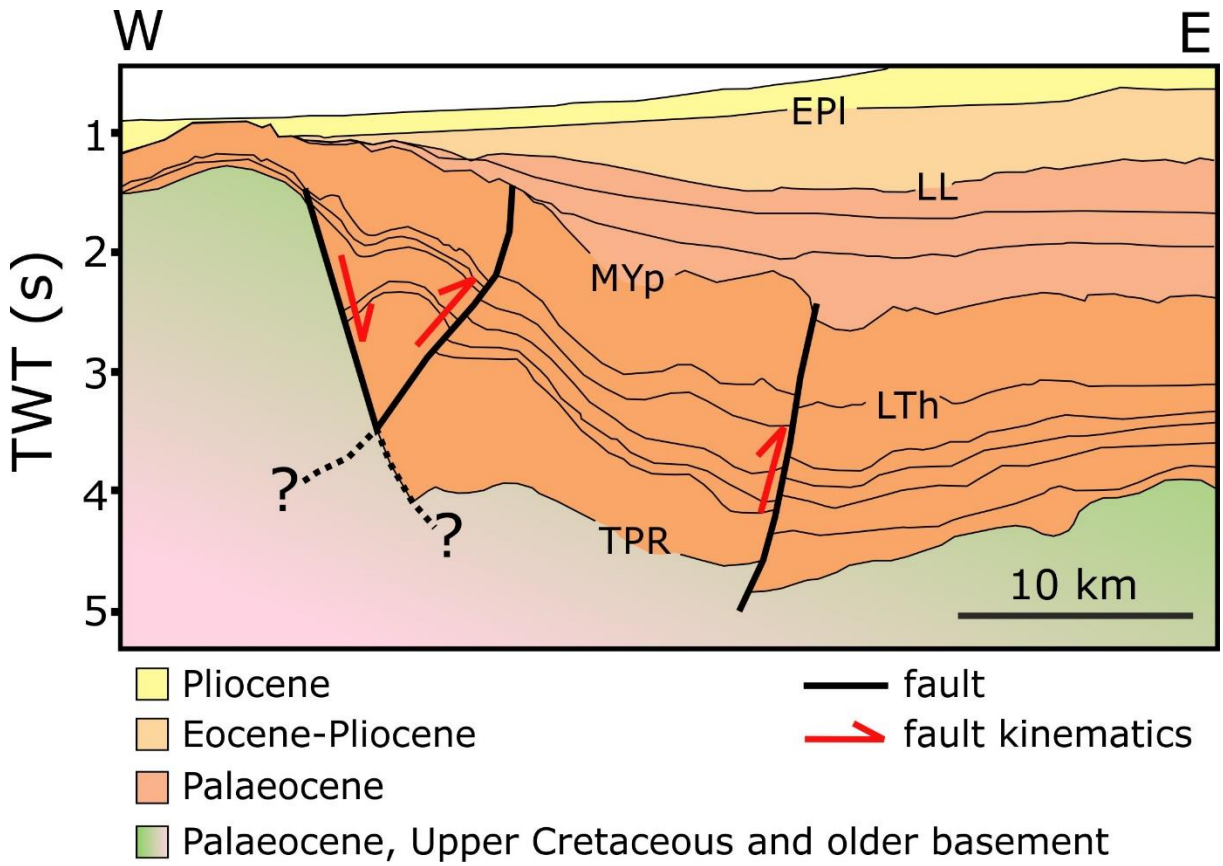

Figure 3. Interpreted seismic line from the Davis Strait, offshore West Greenland, depicting Eocene inversion, modified from Peace et al. (2017). EPl – early Pliocene, MYp – middle Ypresian (early Eocene), LTh – Late Thanetian (late Palaeocene), LL – Late Lutetian (middle Eocene), TPR – Top Pre-Rift. Location on Figure 2a.

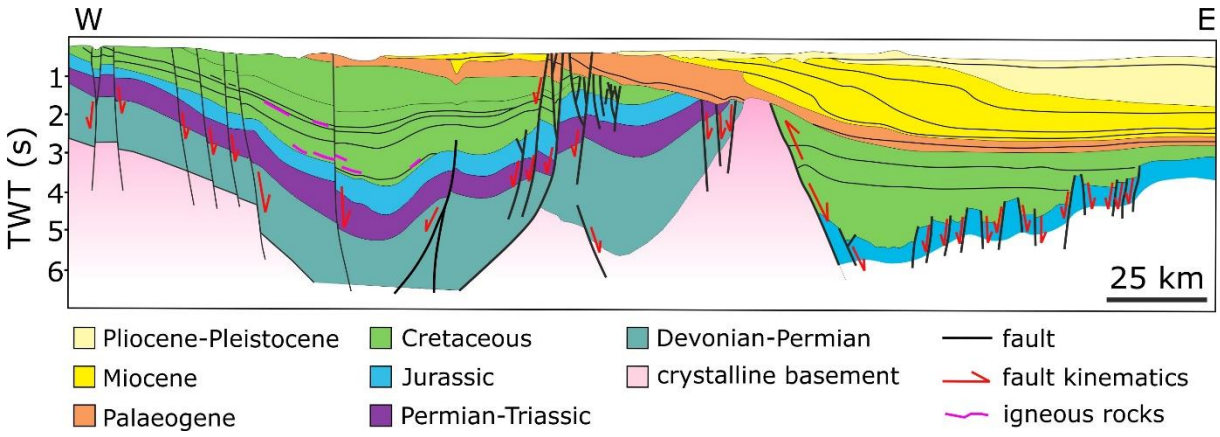

1672

1673

1674 Figure 4. East Greenland margin, Greenland Sea, showing post-Palaeogene inversion as well as older
1675 inversion events, from Hamann et al. (2005). Location on Figure 2a.

1676

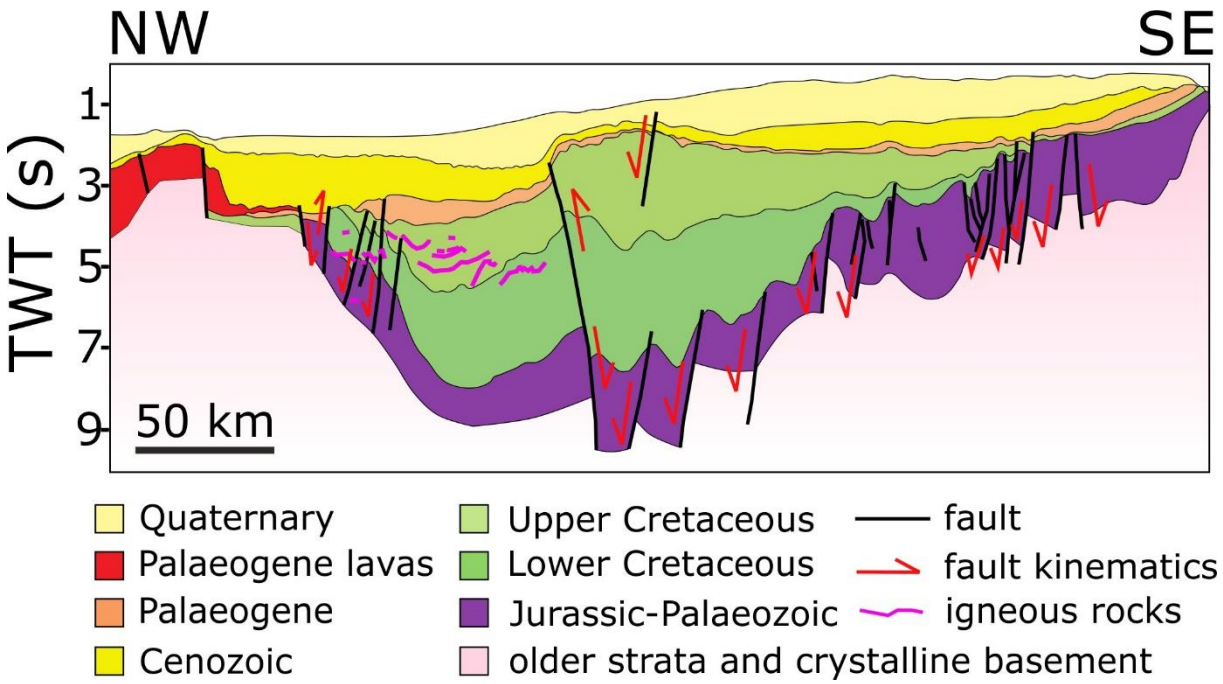

1677

1678

1679 Figure 5. Interpreted seismic line crossing the Helland-Hansen Arch in the Vøring Basin on the
1680 Norwegian margin showing multiple phases of inversion, modified from Stoker et al. (2014). Location
1681 on Figure 2a.

1682

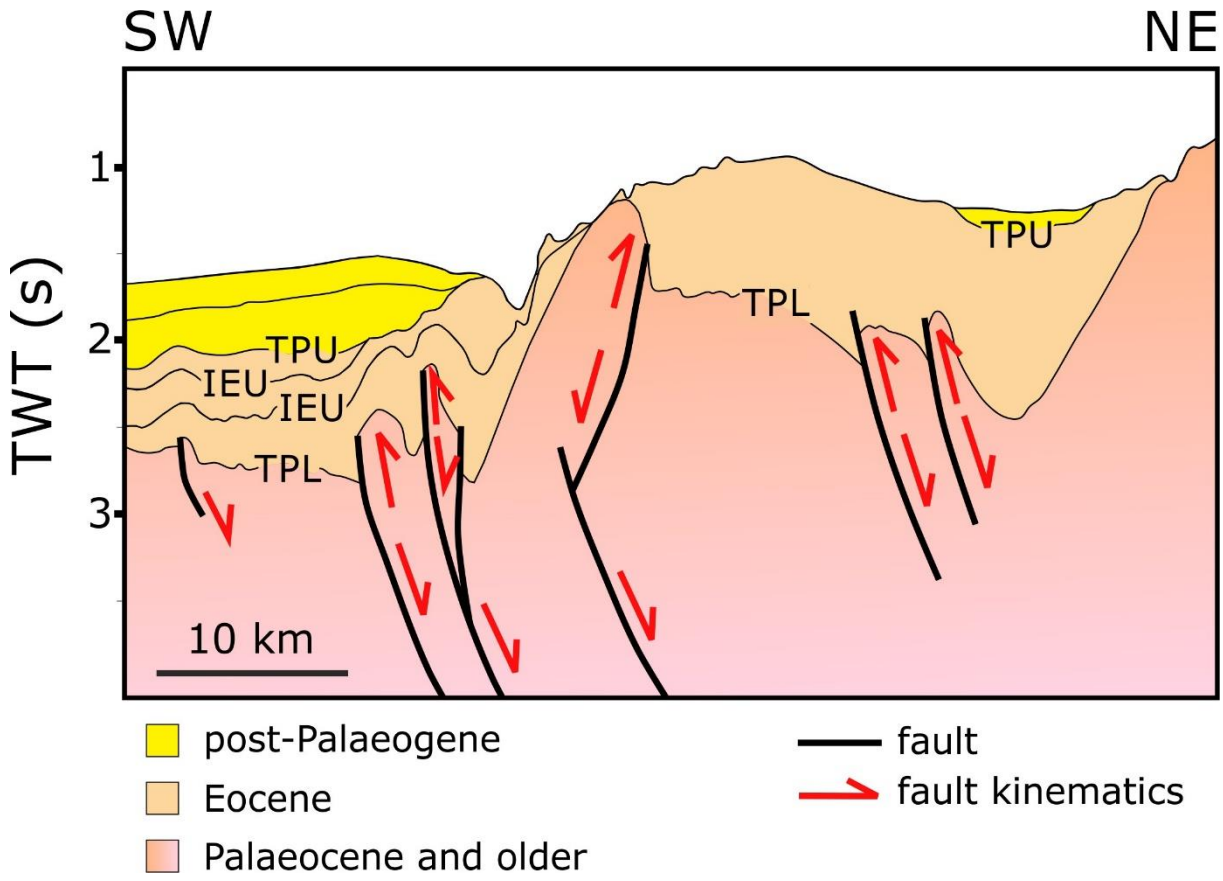

1683

1684

1685 Figure 6. Interpreted seismic line from the Ymir Ridge/Wyville-Thomson Ridge area, NE Rockall Basin
1686 modified from Johnson et al. (2005). TPL = Top Palaeocene lava, IEU = Intra Eocene Unconformities,
1687 TPU = Top Palaeogene Unconformity. Location on Figure 2a.

1688

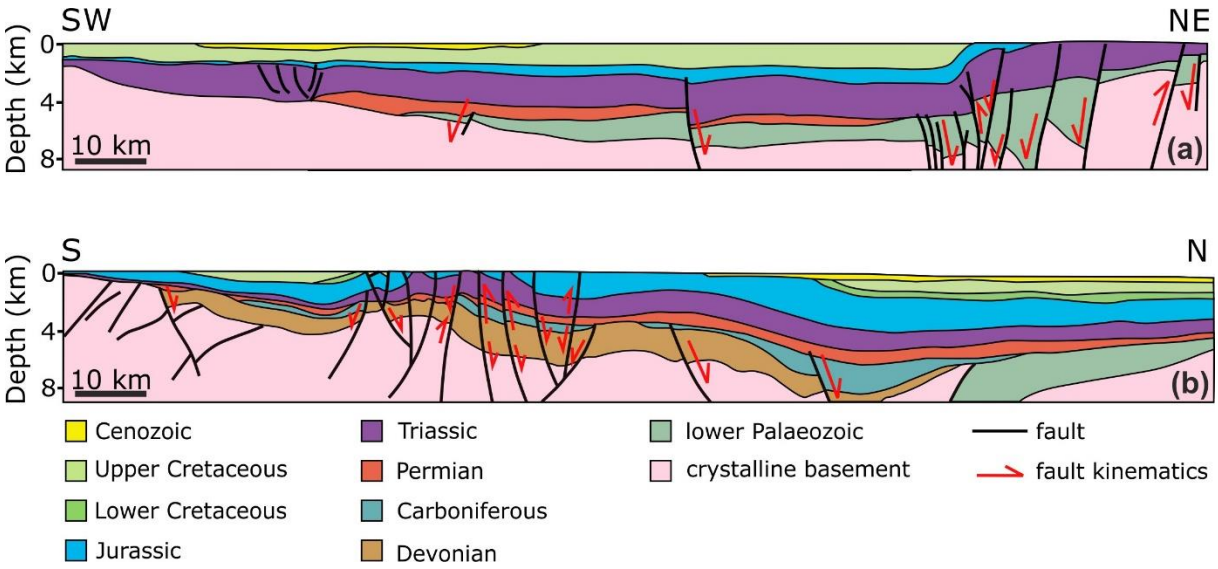

1689

1690

1691 Figure 7. (a) Interpreted seismic line from the Sorgenfrei-Tornquist Zone, Danish Basin, modified
1692 from and (b) Interpreted seismic line from the Tornquist-Tesseyre Zone, Polish Basin, both modified
1693 from Ziegler (1990). Locations on Figure 2a.

1694

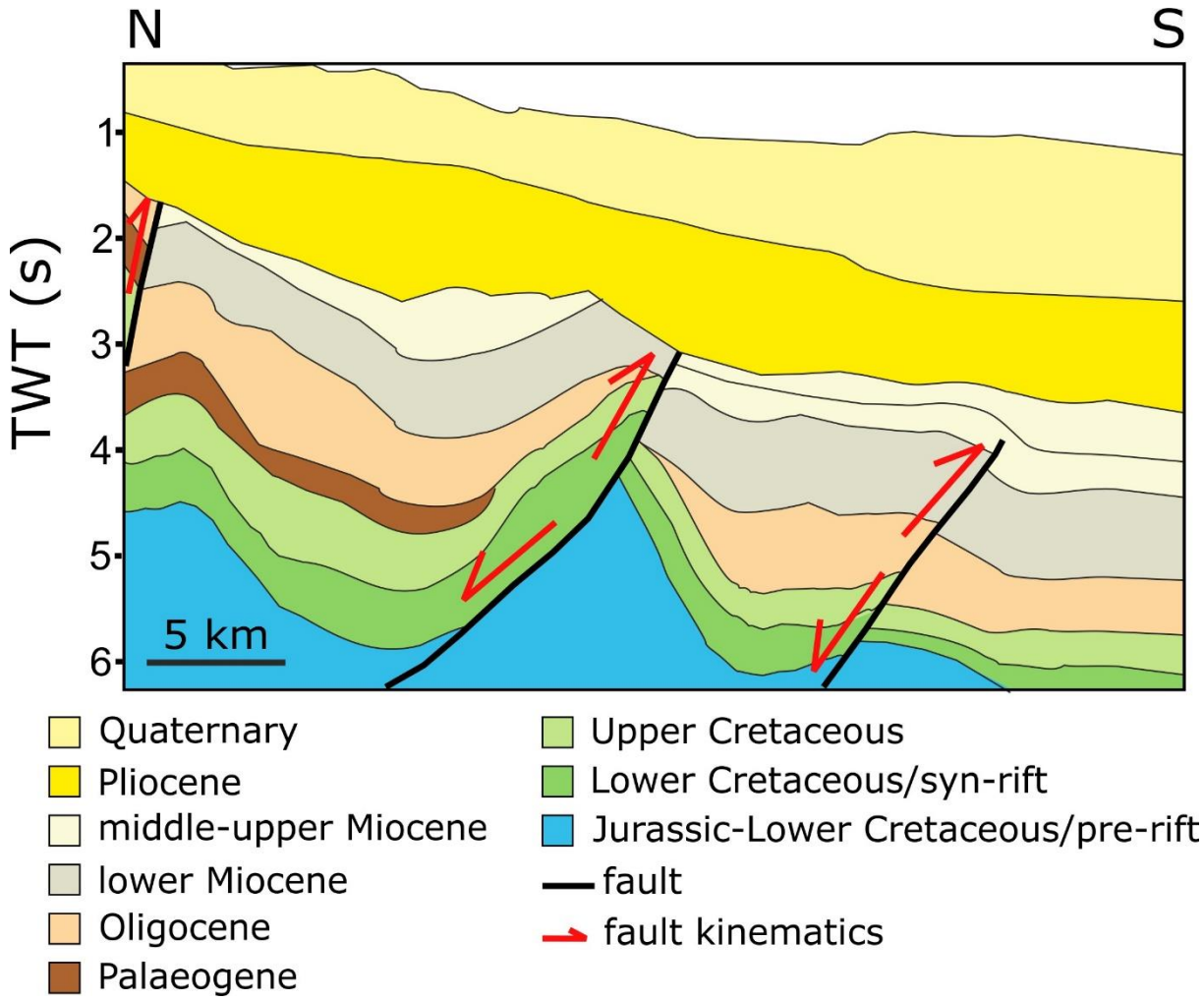

Figure 8. Fragment of an interpreted seismic line from the Crimean Peninsula shelf of the eastern Black Sea Basin, showing post-early Miocene inversion (S.M. Stovba, personal communication; cf. Stovba et al., 2017a,b). Location on Figure 2a.

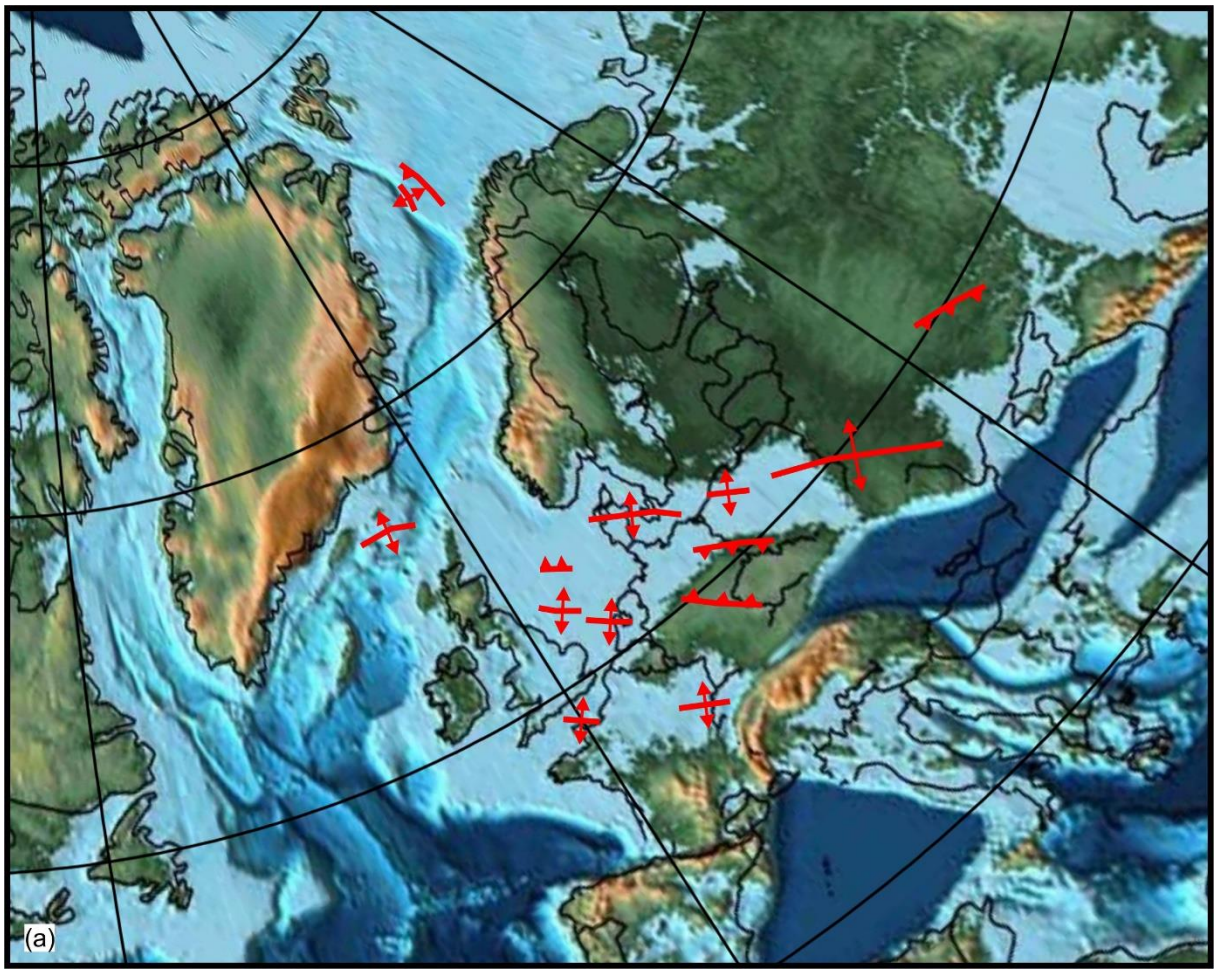

Figure 9a. Generalised pattern of occurrence and orientation of basin inversion structures at 70 Ma ("Late Cretaceous-Palaeocene"), based on the literature cited in section 2, plotted on the relevant palaeotectonic reconstruction (Fig. 10-A4). The anticline symbols generally imply structures buried in the subsurface at the time of formation and the thrust symbols those that displaced the surface at the time of formation. The implied direction of shortening during basin inversion in both cases is, as usual, perpendicular the trend of the axes and thrusts. The topographic reconstruction is based on Scotese's (2016) PALEOMAP PaleoAtlas for GPlates.

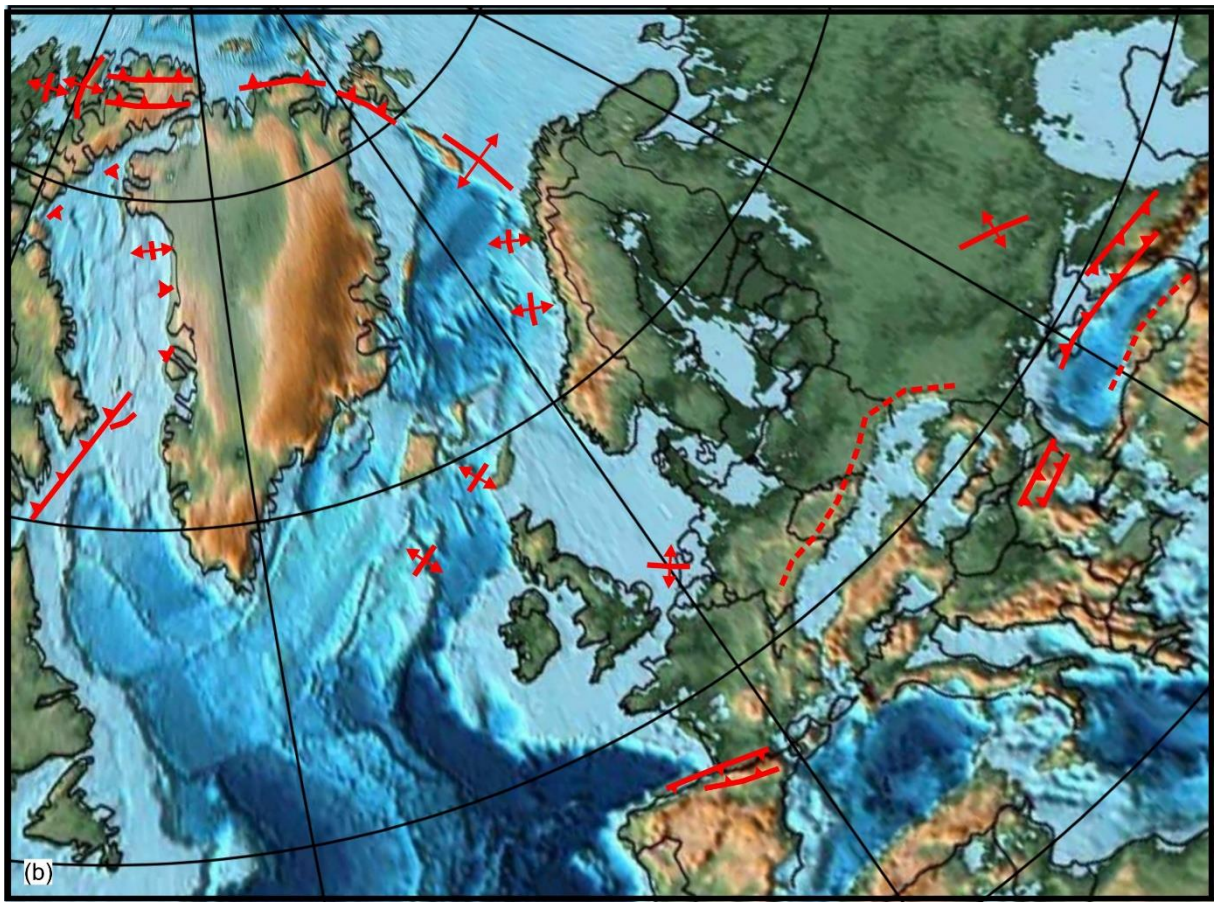

Figure 9b. Generalised pattern of occurrence and orientation of basin inversion structures at 40 Ma ("Eocene-Oligocene"), based on the literature cited in section 2, plotted on the relevant palaeotectonic reconstruction (Fig. 10-A3). The anticline symbols generally imply structures buried in the subsurface at the time of formation and the thrust symbols those that displaced the surface at the time of formation. The implied direction of shortening during basin inversion in both cases is, as usual, perpendicular the trend of the axes and thrusts. The topographic reconstruction is based on Scotese's (2016) PALEOMAP PaleoAtlas for GPlates. The dashed lines give an impression of the Alpine-Tethys belt active deformation front.

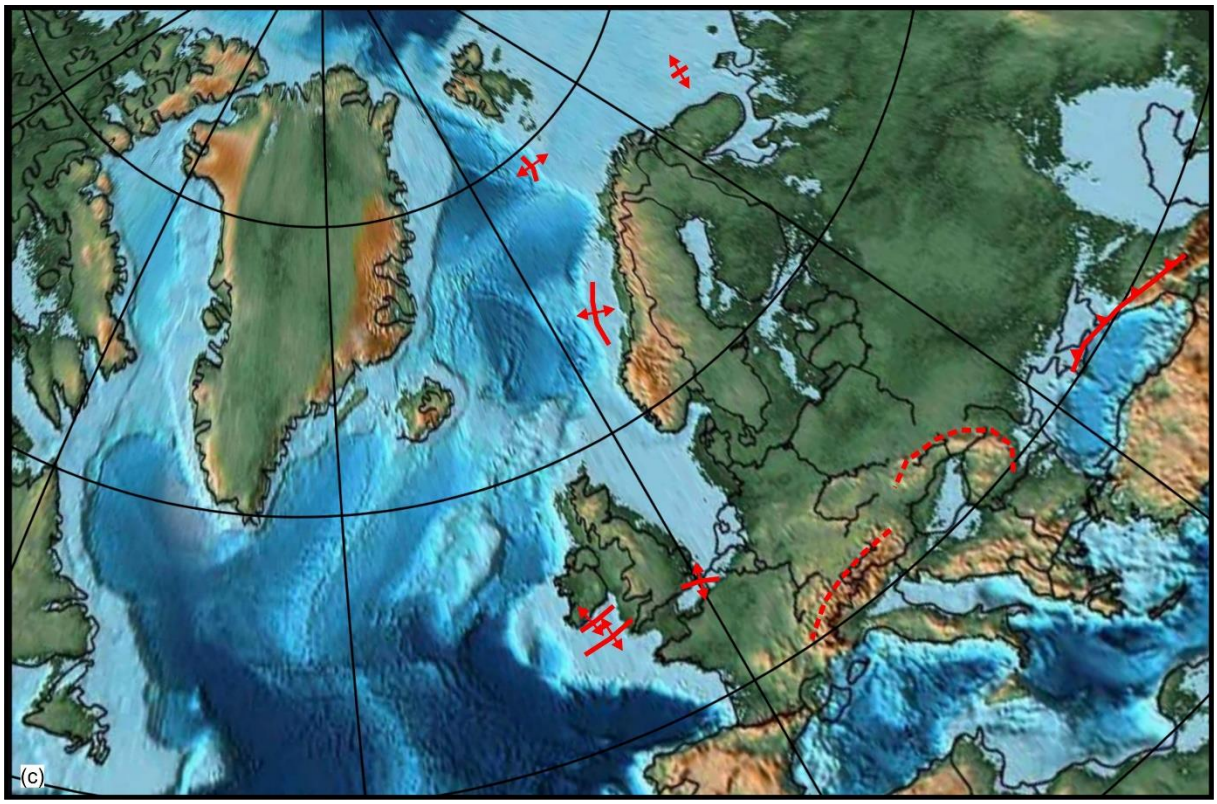

Figure 9c. Generalised pattern of occurrence and orientation of basin inversion structures at 15 Ma ("Miocene"), based on the literature cited in section 2, plotted on the relevant palaeotectonic reconstruction (Fig. 10-A2). The anticline symbols generally imply structures buried in the subsurface at the time of formation and the thrust symbols those that displaced the surface at the time of formation. The implied direction of shortening during basin inversion in both cases is, as usual, perpendicular the trend of the axes and thrusts. The topographic reconstruction is based on Scotese's (2016) PALEOMAP PaleoAtlas for GPlates. The dashed lines give an impression of the Alpine-Tethys belt fossil deformation front in central Europe.

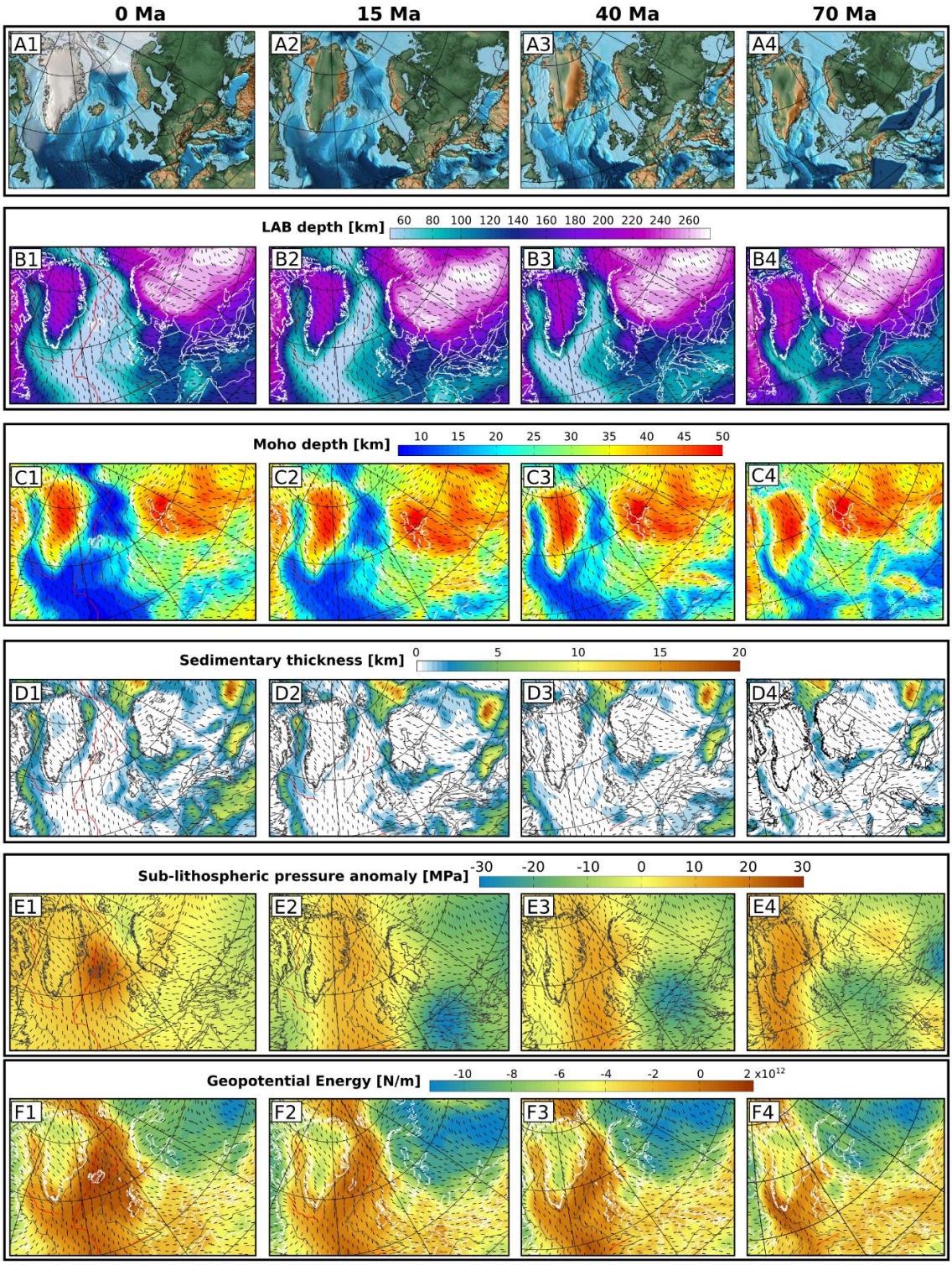

Figure 10. Plate reconstructions (row A) and input data (rows B-F) used in the GP palaeostress modelling for times 0 Ma, 15 Ma, 40 Ma and 70 Ma (columns 1-4, respectively). See the text for more details (section 3.2). The background lines represent the direction of the most compressional principal stress of the total GP stress field for each model time, computed at each model element, extracted from a spherical, 3D global model. Note that the palaeotopographic maps (row A) are for visualisation only and use a slightly different palaeogeographic reconstruction (Scotese, 2016) than the input grids for the GP stress modelling (Seton et al., 2012).

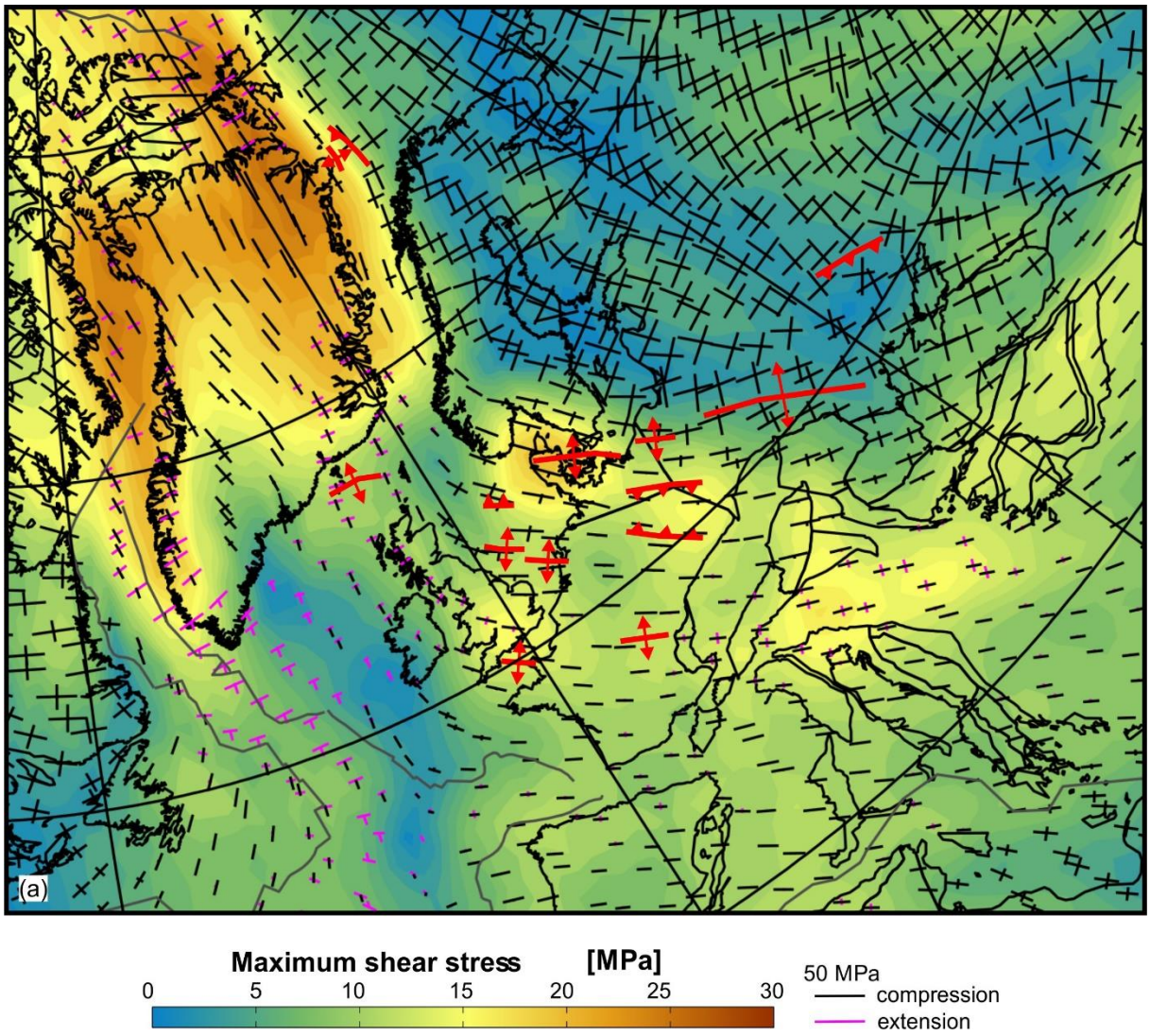

1742

1743

1744 Figure 11a. Generalised pattern of occurrence and orientation of basin inversion structures at 70 Ma
1745 ("Late Cretaceous-Palaeocene"), based on the literature cited in section 2 (and copied from Fig. 9a),
1746 superimposed on computed GP palaeostress results for 70 Ma expressed as principal horizontal
1747 stresses (black lines representing compression and magenta extension) and the magnitude of the
1748 maximum shear stress (red-blue colour bar), which is the difference between maximum (most
1749 extensional) and minimum (most compressional) of the principal horizontal stress components.

1750

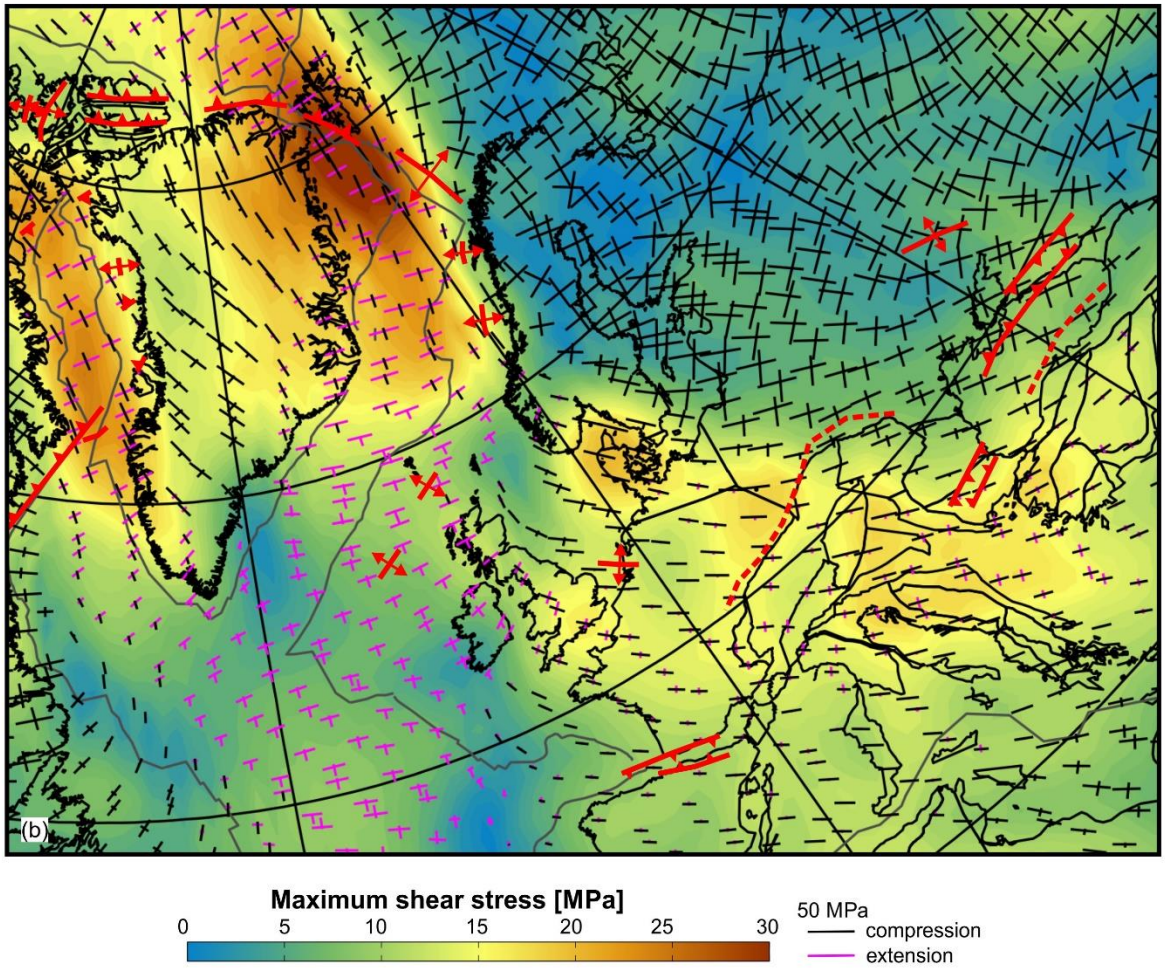

Figure 11b. Generalised pattern of occurrence and orientation of basin inversion structures at 40 Ma ("Eocene-Oligocene"), based on the literature cited in section 2 (and copied from Fig. 9b), superimposed on computed GP palaeostress results for 40 Ma expressed as principal horizontal stresses (black lines representing compression and magenta extension) and the magnitude of the maximum shear stress (red-blue colour bar), which is the difference between maximum (most extensional) and minimum (most compressional) of the principal horizontal stress components.

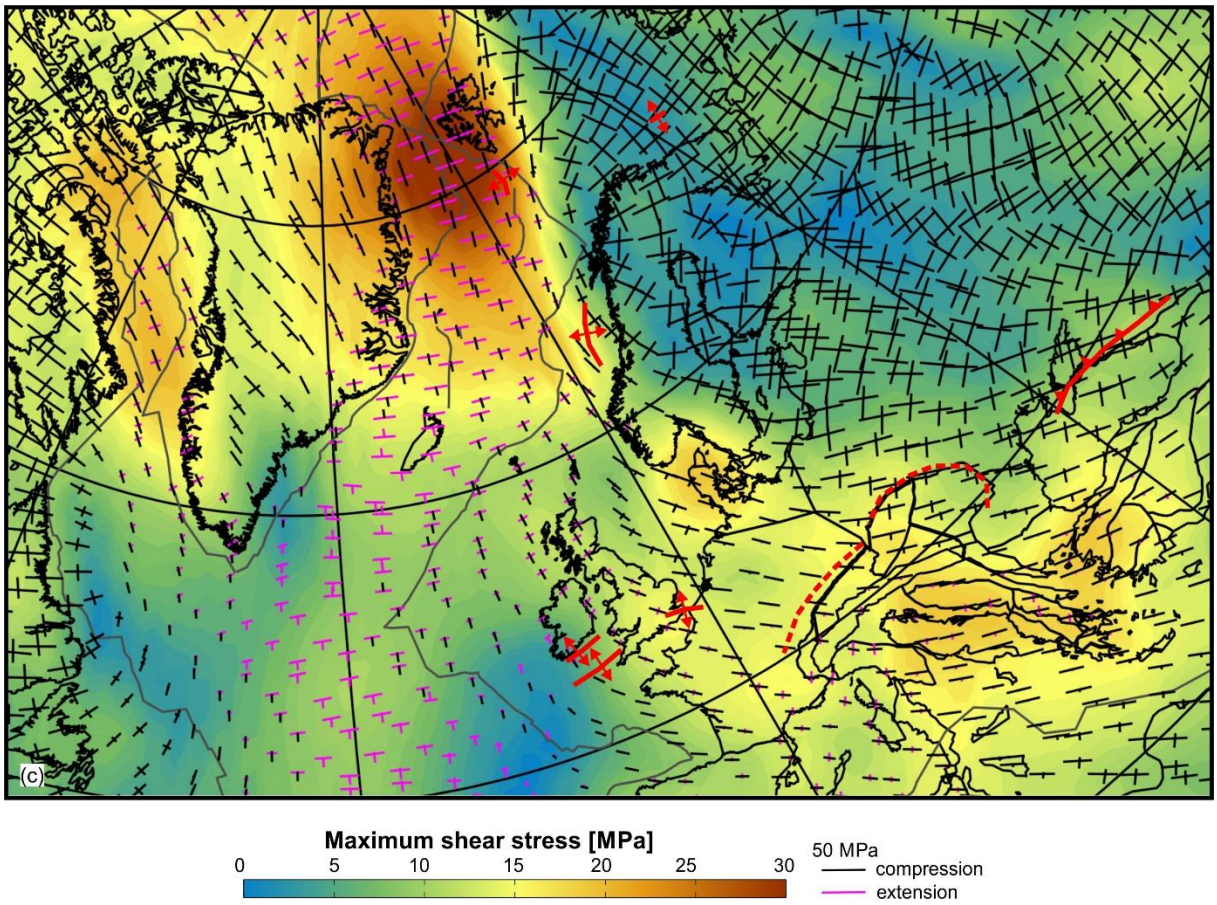

Figure 11c. Generalised pattern of occurrence and orientation of basin inversion structures at 15 Ma ("Miocene"), based on the literature cited in section 2 (and copied from Fig. 9c), superimposed on computed GP palaeostress results for 15 Ma expressed as principal horizontal stresses (black lines representing compression and magenta extension) and the magnitude of the maximum shear stress (red-blue colour bar), which is the difference between maximum (most extensional) and minimum (most compressional) of the principal horizontal stress components.